**MCAT Institute
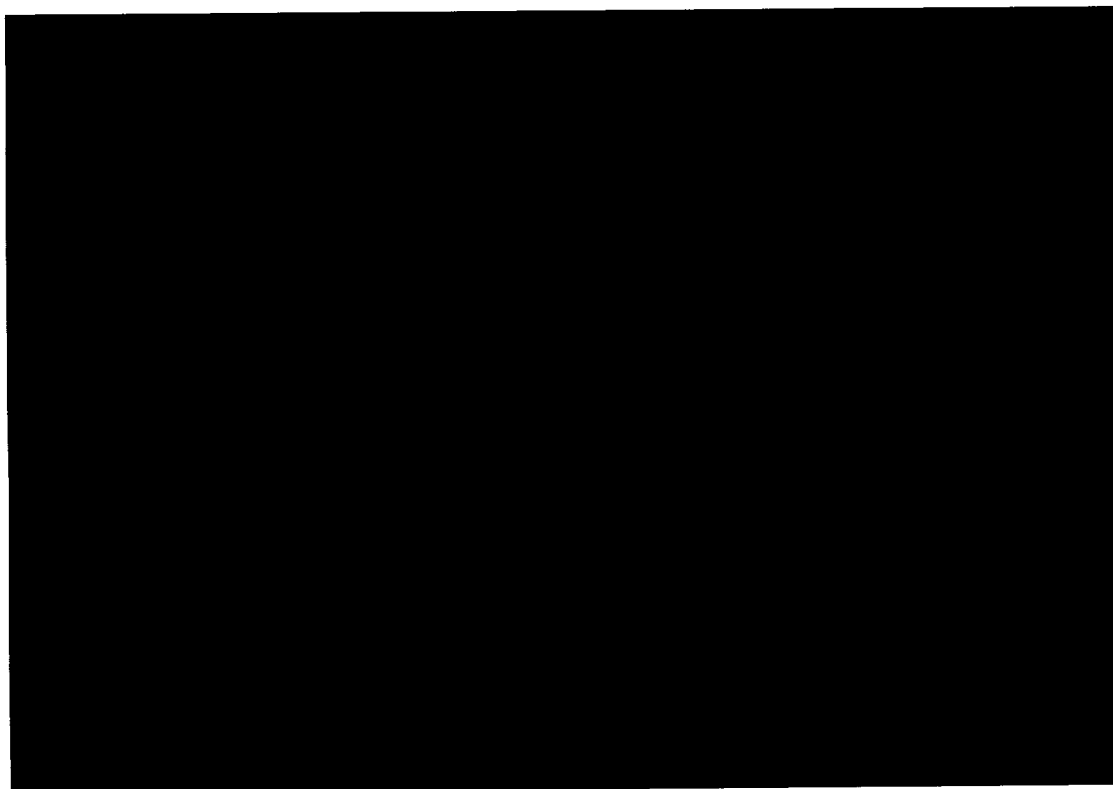Annual Report
94-08**

Parallel Aeroelastic Computations

For Wing and Wing-Body Configurations

Chansup Byun

July 1994

NCC2-740

**MCAT Institute
3933 Blue Gum Drive
San Jose, CA 95127**

PARALLEL AEROELASTIC COMPUTATIONS
FOR WING AND WING-BODY CONFIGURATIONS

Chansup Byun
MCAT Institute

July 1994

1

DIRECT COUPLING OF FLUIDS AND STRUCTURES
FOR AEROSPACE APPLICATIONS

I. INTRODUCTION

In recent years, significant advances have been made for single disciplines in both computational fluid dynamics (CFD) using finite-difference approaches[1] and computational structural dynamics (CSD) using finite-element methods (see Chapter I of Ref. 2). For aerospace vehicles, structures are dominated by internal discontinuous members such as spars, ribs, panels and bulkheads. The finite-element (FE) method, which is fundamentally based on discretization, has proven to be computationally efficient to solve aerospace structures problems. The external aerodynamics of aerospace vehicles is characterized by field discontinuities such as shock waves and flow separations. Finite-difference (FD) computational methods have proven to be efficient to solve such problems.

However, only a limited amount of work has been completed in coupling these two disciplines for multidisciplinary applications. The prime reason is the lack of computational power for combining the two major computational fields. The development of a new generation of parallel computers can possibly alleviate the restriction of computational power.

In addition, such coupling procedures result in an increased level of complication. Therefore, aeroelastic analysis has been mostly performed by coupling advanced computational fluid dynamics (CFD) methods with simple structural modal equations or advanced computational structural dynamics (CSD) methods with simple flow solutions. However, these approaches can be less accurate for the aeroelastic analysis of practical problems such as a full aircraft configuration in the transonic regime. Moreover aeroelastic problems of aerospace vehicles are often dominated by large structural deformations and high flow nonlinearities. It is necessary to develop a fully coupled procedure utilizing advanced computational methods for both disciplines.

The objective of this research is to develop computationally efficient methods for solving fluid-structural interaction problems by directly coupling finite difference Euler/Navier-Stokes equations for fluids and finite element dynamics equations for structures on parallel computers. This capability will significantly impact many aerospace projects of national importance such as Advanced Subsonic Civil Transport (ASCT), where the structural stability margin becomes very critical at the transonic region. This research effort will have direct impact on the High Performance Computing and Communication (HPCC) Program of NASA in the area of parallel computing.

II. PREVIOUS STATUS

A multidisciplinary code for computing unsteady flows and aeroelastic responses of aerospace vehicles, ENSAERO, has been developed on serial supercomputers at the Computational Aerosciences Branch of the NASA Ames Research Center.[3] This multidisciplinary code computes unsteady aerodynamic responses of aircraft using the Euler/Navier-Stokes equations. An aeroelastic shape-conforming moving grid is used to include the effect of structural deformations on unsteady flows. This code is designed in a modular fashion to adopt several different numerical schemes suitable for accurate aeroelastic computations. The basic coding of ENSAERO can accommodate zonal grid techniques for efficient modeling of full aircraft.

An early version of ENSAERO[4] has been successfully applied in computing aeroelastic responses of a rectangular wing by using the Euler equations for fluids and the modal equations for structures. The result demonstrates that the code can accurately predict the flutter dynamic pressure of a rectangular wing. The code was extended to compute aeroelastic responses using the Navier-Stokes equations for fluids.[5] Later, it was updated by utilizing an upwind algorithm, and the code has been applied to fighter wings undergoing unsteady motions[6,7] at moderately large angles of attack. This code also has a capability of modeling moving control surfaces.[8] Furthermore, ENSAERO has demonstrated the capability to simulate transonic flows on wing-body configurations using the Navier-Stokes equations.[9]

In the past, the modal equations were used to model structures for the purpose of aeroelastic analysis. For simple geometries such as clean wings, the modal approach can produce accurate response results. However, the modal approach may be less accurate for complex structures such as wing-body configurations. In order to accurately represent aeroelastic responses of general wing-body configurations, the modal equations should be replaced with the finite element equations. Recently, a typical wing-body configuration has been used to demonstrate aeroelastic responses at transonic Mach numbers using the Navier-Stokes equations for fluids and the finite element equations for structures.[10] Simple one-dimensional beam elements are used to model the wing-body structures. Each node has three degrees of freedom (DOF) corresponding to transverse displacement and to transverse and torsional rotations, respectively.

Recently, a version of ENSAERO[11] that uses the Euler equations for fluids and the modal equations for structures has been parallelized on the Intel iPSC/860 at Ames. The Intel iPSC/860 is a distributed-memory, multiple-instruction, multiple-data (MIMD) computer with 128 processors. In this parallel implementation, a domain decomposition approach is used in which the fluid equations and the structural equations are modeled in separate computational domains. Each domain is mapped individually onto a group of processors, referred to as a cube on the Intel iPSC/860. However, because of the coupling between the disciplines, there is a need to exchange data, such as pressures and structural deformations at interfaces. This exchange between the fluid and structural domains is accomplished through an intercube communication mechanism,[12] which enables different processors in each cube to communicate directly.

3

III. CURRENT WORK

1. Finite Element Modeling of Structures

The finite element representation of structures generally provides more accurate modeling of structures than the modal representation does in aeroelastic computations. For the aeroelastic computations of wing and wing-body structures, plate and shell models are used as shown in Appendix A and C. The parallel implementation of the structural domain is mainly discussed in Appendix B. Although the current implementation is only using ANS4 plate/shell elements to model structures, it is possible to use different types of elements.

2. Fluid-Structural Interface

In aeroelastic analysis, it is necessary to represent the equivalent aerodynamic loads at the structural nodal points and to represent the deformed structural configurations at the aerodynamic grid points. In the present domain decomposition approach, coupling between the fluid and structural domains is achieved by interfacing the boundary data, such as aerodynamic pressures and structural deflections, at each time step. An analytical moving-grid technique has been successfully used to deform the aerodynamic grid according to the structural deflections at the end of every time-step.[3,4,10] There are different approaches for obtaining the external load vector, depending on the equations used for the structural dynamic analysis.

In order to replace modal equations with finite element structural dynamics equations for fluid-structural interaction problems, a new fluid-structural interface, similar to the modal matrix used for modal equations, should be developed. Several numerical procedures have been developed for exchanging the necessary information between the fluid and structural domains.[13-15] In this research, two different types of fluid-structural interfaces were studied and compared as shown in Appendix A.

The current implementation of the fluid-structural interface on the Intel iPSC/860 is based on direct node-to-node communication. Thus each of precessors assigned to the fluid domain can communicate with any processors of the structural domain. Figure 1 show the typical communication patern obtained during the aeroelastic computation of a High Speed Civil Transport (HSCT) model on the Intel iPSC/860. More details are found in Appendix C.

3. Parallel Integration

In a serial computer, the integration of both fluid and structural equations is performed one after the other in a sequential nature. Figure 2(a) shows the sequential integration scheme on serial computers. When implementing the integration scheme on parallel computers, all processors can be used to solve the fluid and structural equations sequentially

as shown Fig. 2(b). But this approach requires more memory per processor and two disciplines have to be implemented in a single program. As a result, modularity of each algorithm for individual disciplines will have to be sacrificed to a significant degree. In addition, this approach will be less efficient as increasing the number of processors because the problem is not linearly scaled.

However, while keeping modularity of each discipline, computations can be done more efficiently on MIMD parallel computers by executing the integration of both fluid and structural equations concurrently as shown in Fig. 2(c). In the proposed parallel integration scheme, both domains start computations independently and one of the solvers waits until the other finishes its calculation. Then they exchange the required data with each other for the next time step. By doing so, the parallel integration can reduce the idle time since only one cube (the fastest) will have to wait. This integration scheme exploits the parallelism offered by the domain decomposition approach to solve the coupled fluid-structural interaction problems.

4. Computational Results

Aeroelastic computations for the NASA Langley Clipped Delta Wing were performed first on a Cray Y-MP serial computer and then on the Intel iPSC/860 MIMD parallel computer. Figure 3 shows highly deformed wing due to the fluid-structural interactions. The surface is colored by pressure coefficient. Comparison between the modal and finite element analyses for structures and accuracy of the interfaces considered in this research are given in Appendix A.

Computational performance results are found in Appendix B. Including the data exchange between fluid and structural domains, the current aeroelastically deforming grid scheme requires about 12 percent of the computational time per each integration step.

Application of the procedure to wing-body configurations can be found in Appendices A and C. Aeroelastic computations are done on flexible wing and body structures. Figure 4 shows highly deformed Boeing 1807 HSCT model due to the fluid-structural interactions. The surface is colored by pressure coefficient.

IV. SUMMARY AND CONCLUSIONS

In this work, a procedure to compute aeroelastic responses on MIMD parallel computers using direct coupling of the finite difference Euler/Navier Stokes equations for fluids and the finite element dynamics equations for structures is developed for wing and wing-body structures. The procedure is based on a domain decomposition approach which enables algorithms for the fluid and structural disciplines to be developed and maintained independently. This approach provides an efficient and effective environment to researchers. A researcher working in the fluid or the structural discipline can develop his own algorithms independent of the others. The only thing to be done together is coupling of the disciplines. Since coupling of the disciplines is achieved by exchanging boundary data through

an intercube communication mechanism that does not interfere with interprocessor communication within a cube, coupling should not cause any problem, This makes it easy for each discipline to incorporate and develop new algorithms or data structures without interferences.

The performance of the structural domain is far behind that of the fluid domain. This is due to the less desirable performance of the JPCG algorithm. It is noted that direct solvers are still in the early stages of development. However, since the procedure developed here allows for one domain to select algorithms independent of others, the JPCG algorithm can be easily replaced with more efficient algorithms when available. Although the solver for the structure is not efficient on a serial computer, reasonable computational speed and a good load balance can be achieved by assigning more processors to the structural domain. The overall time per integration step of parallel ENSAERO using 96 processors on the iPSC/860 is reduced to about 60% of the best time obtained on a single Y-MP processor for the particular problem considered. This shows the advantage of using the domain decomposition approach for the multidisciplinary analysis on MIMD parallel computers.

In addition, a parallel integration procedure is developed to solve fluid and structural equations together. The parallel integration scheme enables the combination of advanced CFD and CSD technologies with minimal increase in computational time per integration step while keeping modularity of each discipline. The time per integration step is solely determined by the domain that requires most computational time on the iPSC/860. This parallel integration is one of the advantages of using MIMD computers for multidisciplinary analysis. The procedure developed in this research will provide an efficient tool for solving aeroelastic problems of complete aerospace vehicle configurations on MIMD computers.

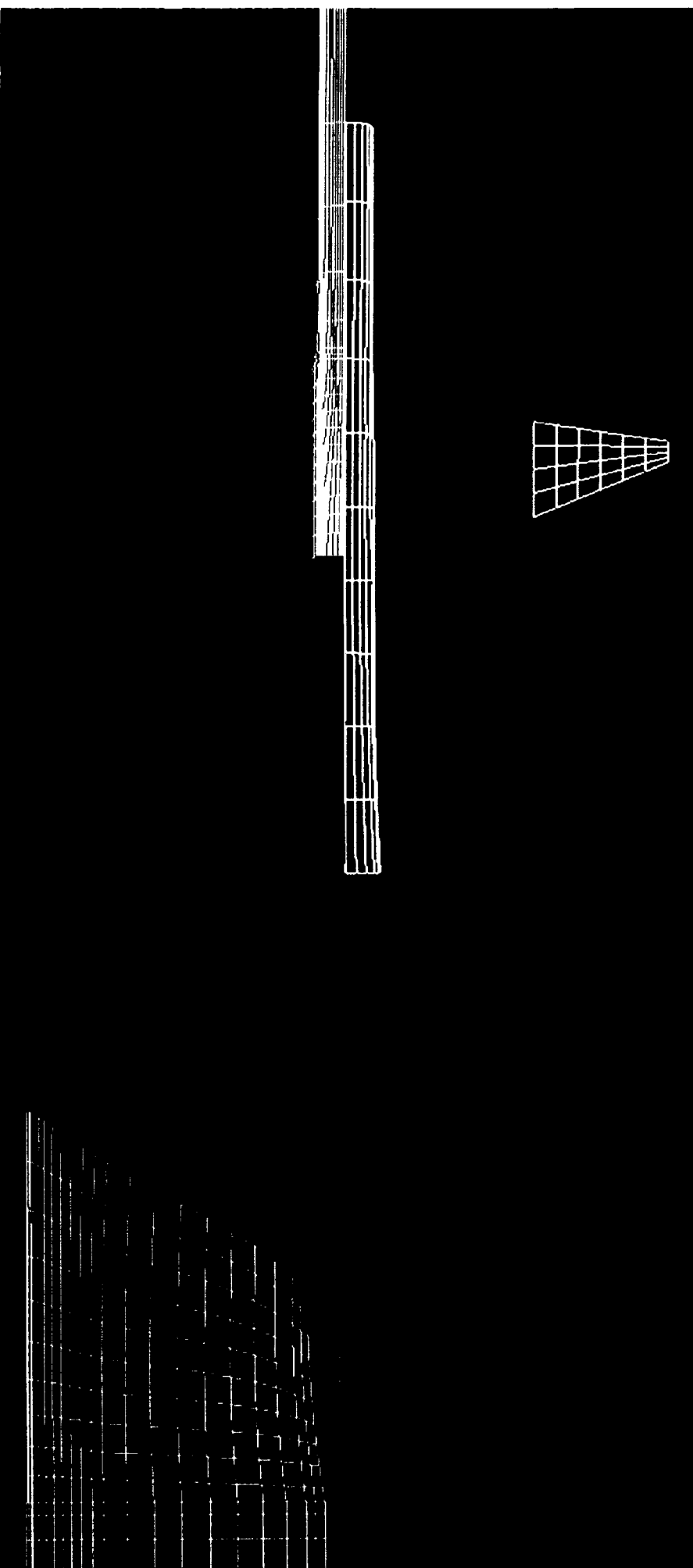Based on this work the following conclusions can be made.

1. It is feasible to directly couple the finite difference flow equations and finite element structural equations to obtain accurate results, though each discipline is solved in a separate computational domain. This domain decomposition approach takes advantage of efficient methods developed for each individual discipline.

2. The use of finite element structures in place of modal structures produces more accurate and detailed results.

3. This domain decomposition approach is suitable for parallel computers. However, the structural domain requires a more efficient solver for the application of larger size problems.

ACKNOWLEDGMENTS

REFERENCES

1. Holst, T. L, Flores, J., Kaynak, U., and Chaderjian, N. , "Navier-Stokes Computations, Including a Complete F-16 Aircraft," Chapter 21, Applied Computational Aerodynamics, edited by P. A. Henne, Vol. 125, *Progress in Astronautics and Aeronautics*, AIAA, ISBN 0-930403-69-X, 1990.

2. Yang, T. Y., *Finite Element Structural Analysis*, Prentice-Hall, Inc., Englewood Cliffs, New Jersey, 1986.

3. G. P. Guruswamy, "ENSAERO - A Multidisciplinary Program for Fluid/ Structural Interaction Studies of Aerospace Vehicles," *Computing Systems Engineering*, Vol. 1, 1990, pp. 237–256.

4. G. P. Guruswamy, "Unsteady Aerodynamic and Aeroelastic Calculations for Wings Using Euler Equations," *AIAA J.*, Vol. 28, 1990, pp. 461–469.

5. G. P. Guruswamy, "Navier-Stokes Computations on Swept-Tapered Wings, Including Flexibility," AIAA Paper 90-1152, Apr. 1990.

6. S. Obayashi, G. P. Guruswamy and P. M. Goorjian, "Application of Streamwise Upwind Algorithm for Unsteady Transonic Computations over Oscillating Wings," AIAA Paper 90-3103, Aug. 1990.

7. S. Obayashi and G. P. Guruswamy, "Unsteady Shock-Vortex Interaction on a Flexible Delta Wing," AIAA Paper 91-1109, Apr. 1991.

8. S. Obayashi and G. P. Guruswamy, "Navier-Stokes Computations for Oscillating Control Surface," AIAA Paper 92-4431, Aug. 1992.

9. S. Obayashi, G. P. Guruswamy and E. L. Tu, "Unsteady Navier-Stokes Computations on a Wing-Body Configuration in Ramp Motions," AIAA Paper 91-2865, Aug. 1991.

10. G. P. Guruswamy, "Coupled Finite-Difference/Finite-Element Approach for Wing-Body Aeroelasticity," AIAA Paper 92-4680, Sep. 1992.

11. G. P. Guruswamy, S. Weeratunga and E. Pramono, " Direct Coupling Approach to Fluids/Structures Interaction Problems for Parallel Computing," NASA CAS Conference, Moffett Field, CA 94035, Aug. 18-20, 1992, pp. 46–47.

12. E. Barszcz, "Intercube Communication on the iPSC/860," Proceedings of the Scalable High Performance Computing Conference, Williamsburg, VA, April 26-29, 1992, pp. 307–313.

13. R. L. Harder and R. N. Desmarais, "Interpolation Using Surface Spline," *J. of Aircraft*, Vol. 9, 1972, pp. 189–191.

14. K. Appa, "Finite-Surface Spline," *J. of Aircraft*, Vol. 26, 1989, pp. 495–496.

15. R. M. V. Pidaparti, "Structural and Aerodynamic Data Transformation Using Inverse Isoparametric Mapping," *J. of Aircraft*, Vol. 29, 1992, pp. 507–509.

Figure 1. An intercube communication pattern between fluid and structural domains

Sequential approach

Parallel approach

Time

Interface

Interface

Interface

Serial computers

Parallel computers
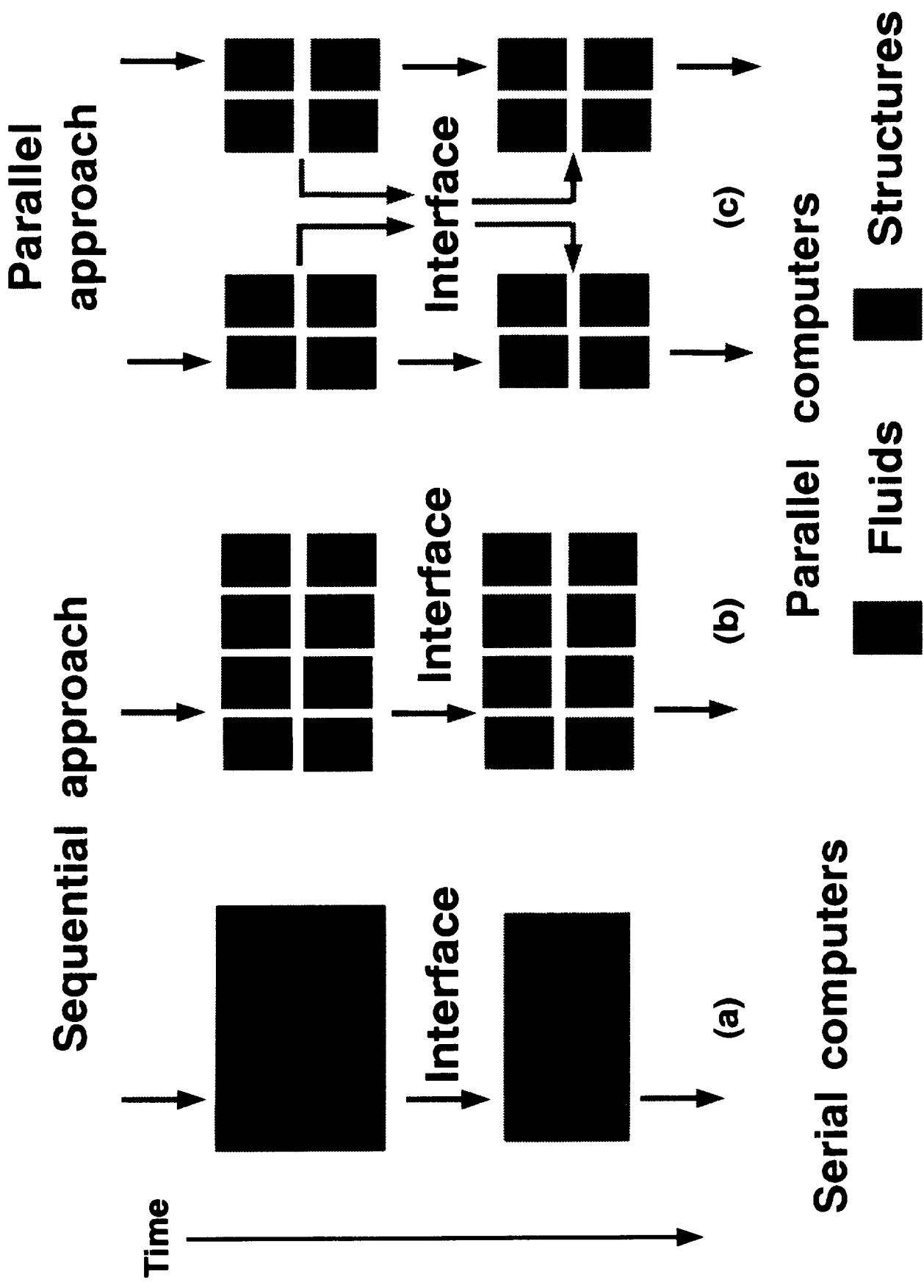
(a)

(b)

(c)

■ Fluids ■ Structures

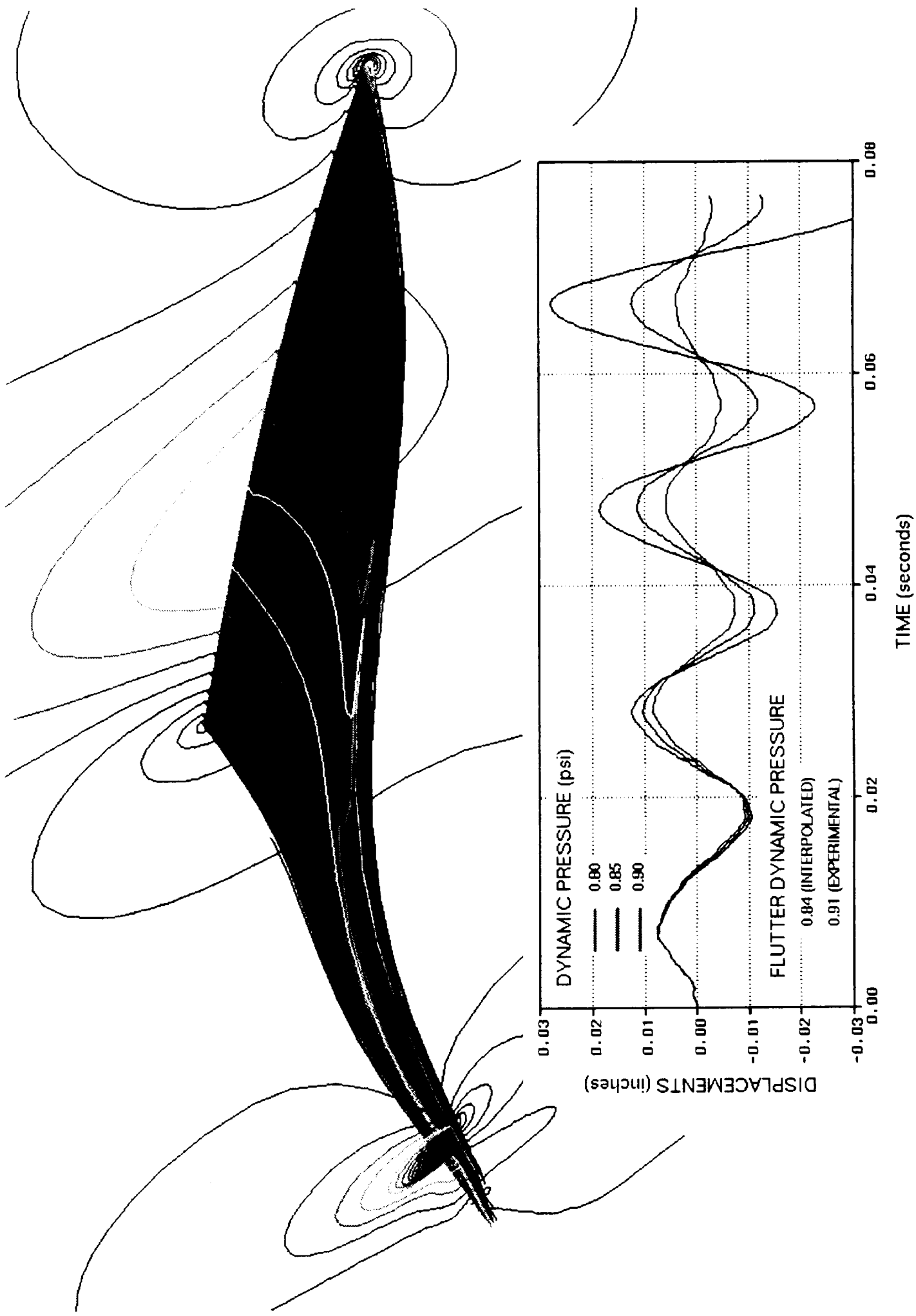# Figure 2. Comparison between integration schemes

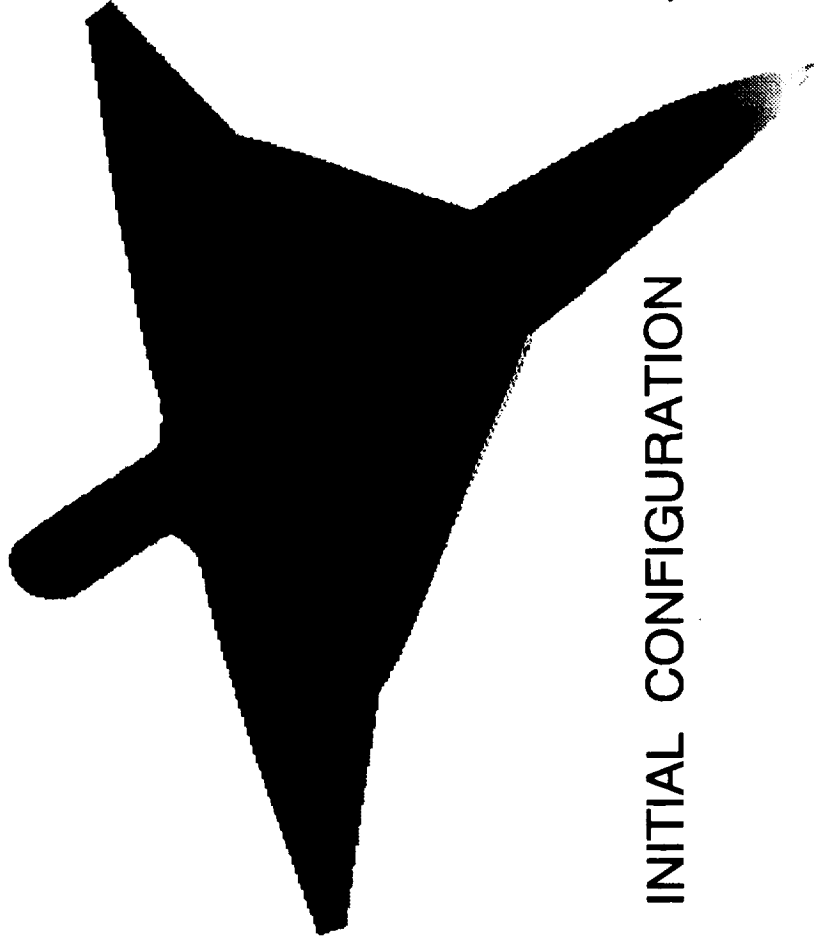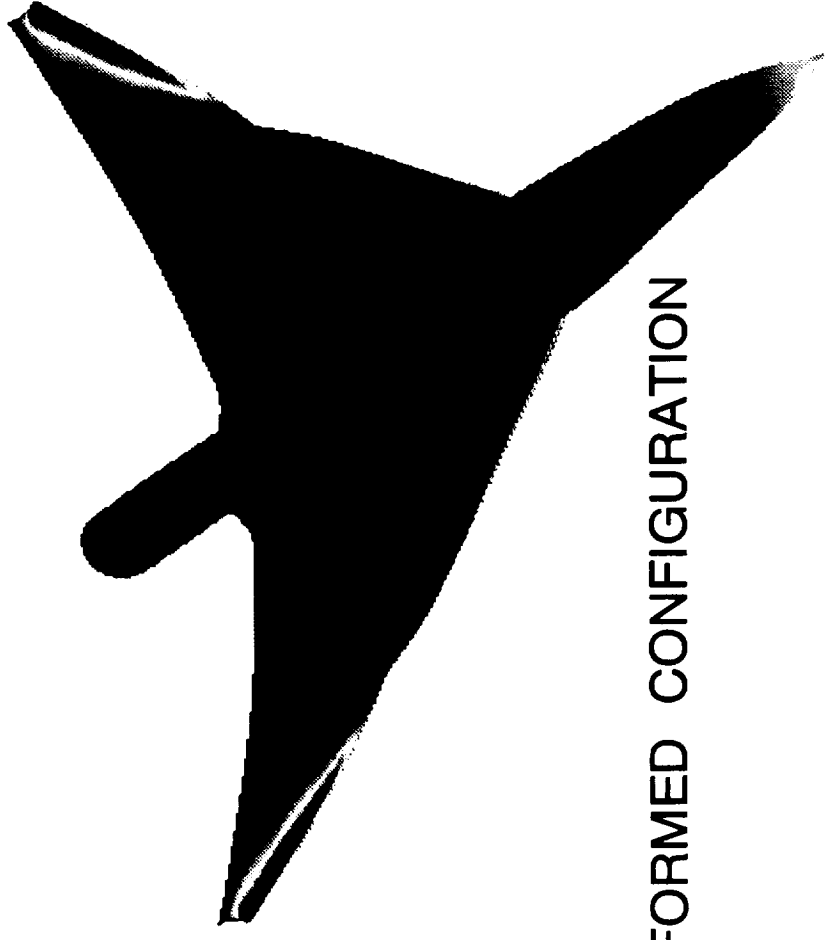Figure 3. Aeroelastic deformation of NASA Langley Clipped Delta wing with pressure contour distribution. Mach number = 0.854, Angle of attack = 0.0 degree, Euler Computation

INITIAL CONFIGURATION

DEFORMED CONFIGURATION

Figure 4. Aeroelastic deformation of Boeing 1807 HSCT model with surface pressure distribution. Mach number = 2.1, Angle of attack = 4.75 degrees, Euler computation

APPENDIX A.

'

AIAA-93-3087

Fluid-Structural Interactions Using Navier-Stokes Flow Equations Coupled with Shell Finite Element Structures

G. P. Guruswamy and C. Byun
NASA Ames Research Center
Moffett Field, CA

AIAA 24th
Fluid Dynamics Conference
July 6-9, 1993/ Orlando, FL

FLUID-STRUCTURAL INTERACTIONS USING NAVIER-STOKES FLOW EQUATIONS COUPLED WITH SHELL FINITE ELEMENT STRUCTURES

Guru P. Guruswamy[*] and Chansup Byun[†]
Computational Aerosciences Branch
NASA Ames Research Center, Moffett Field, California 94035-1000

Abstract

A computational procedure is presented to study fluid-structural interaction problems for three-dimensional aerospace structures. The flow is modeled using the three-dimensional unsteady Euler/Navier-Stokes equations and solved using the finite-difference approach. The three dimensional structure is modeled using shell/plate finite-element formulation. The two disciplines are coupled using a domain decomposition approach. Accurate procedures both in time and space are developed to combine the solutions from the flow equations with those of the structural equations. Time accuracy is maintained using aeroelastic configuration-adaptive moving grids that are computed every time step. The work done by aerodynamic forces due to structural deformations is preserved using consistent loads. The present procedure is validated by computing the aeroelastic response of a wing and comparing with experiment. Results are illustrated for a typical wing-body configuration.

Introduction

In recent years, significant advances have been made for single disciplines in both computational fluid dynamics (CFD) using finite-difference approaches[1] and computational structural dynamics (CSD) using finite-element methods (see Chapter I of Ref. 2). For aerospace vehicles, structures are dominated by internal discontinuous members such as spars, ribs, panels and bulkheads. The finite-element (FE) method, which is fundamentally based on discretization, has proven to be computationally efficient to solve aerospace structures problems. The external aerodynamics of aerospace vehicles is dominated by field discontinuities such as shock waves and flow separations. Finite-difference (FD) computational methods have proven to be efficient to solve such problems.

Problems in aeroelasticity associated with nonlinear systems have been solved using both uncoupled and coupled methods.[3] Uncoupled methods are less expensive but are limited to very small perturbations with moderate nonlinearity. However, aeroelastic problems of aerospace vehicles are often dominated by large structural deformations and high flow nonlinearities. Fully coupled procedures are required to solve such aeroelastic problems accurately.

In computing aeroelasticity with coupled procedures, one needs to deal with fluid equations in an Eulerian reference system and structural equations in a Lagrangian system. Also, the structural system is physically much stiffer than the fluid system. As a result, the numerical matrices associated with structures are orders of magnitude stiffer than those associated with fluids. Therefore, it is numerically inefficient or even impossible to solve both systems using a monolithic numerical scheme.

Guruswamy and Yang[3] presented a numerically accurate and efficient approach to solve this problem for two-dimensional airfoils by independently modeling fluids using FD-based transonic small perturbation (TSP) equations and structures using FE equations and coupling the solutions only at boundary interfaces between fluids and structures. The coupling of solutions at boundaries can be done either explicitly or implicitly. This domain decomposition approach allows one to take full advantage of numerical procedures of individual disciplines such as FD for fluids and FE for structures. This accurate coupling procedure has been extended to three-dimensional problems and incorporated in several advanced aeroelastic codes such as XTRAN3S[4], ATRAN3S[5] and CAP-TSD[6] based on the TSP theory. It was later demonstrated that the same technique can be used by modeling the fluids with Euler/Navier-Stokes equations on moving grids.[7,8] The accuracy of the coupling is maintained by matching the field grid displacements with the structural displacements at the surface. This new development is incorporated in the computer code ENSAERO.[9]

As an alternate to the domain decomposition approach, there have been some attempts to solve both fluids and structures in a single computational domain.[10,11] This single computational domain approach is not new to the researchers dealing with fluid-

---

* Research Scientist, AIAA Associate Fellow
† Research Scientist, MCAT Institute, AIAA Member

1

structural interaction problems. In the late 60's, there were several attempts to solve fluid-structural interaction problems using a single FE computational domain (see Chapter 20 of Ref. 12). The main bottleneck arose from ill-conditioned matrices associated with two physical domains with large variations in stiffness properties. As a result, a subdomain approach was devised where fluids and structures are solved in separate domains and solutions are combined through the boundary conditions similar to the domain-decomposition approach explained above. However, there have been renewed attempts to solve both fluids and structures in a single computational domain for aeroelastic applications. So far, such attempts are limited to simple two-dimensional problems and have not proven to be better than the domain decomposition approach. Because of the lack of comparison with other approaches and details about the computational speed, it is difficult to estimate the scope of these alternate approaches. The drop in the convergence rate from the rigid case to the flexible case in Ref. 11 indicates the weakness of the single domain approach.

In the domain decomposition approach, to date, advanced CFD methods such as those based on the Navier-Stokes equations are used to compute aeroelasticity of simple wings modeled structural equations. The modal approach significantly reduces the number of structural unknowns to a great extent when compared to a direct use of FE equations. For simple geometries such as isolated wings, the modal approach can produce accurate response results. However, it can be less accurate for complex structures such as wing-body configurations. Since the structural properties of the body are considerably different from those of the wing, it is difficult to pre-select the modes to accurately represent the full configuration. Therefore, it is more accurate to directly use FE structural equations. Also, by using the FE equations, stresses and other data that are required for the design can be directly computed in addition to displacement responses.

In this work, the capabilities of ENSAERO are extended to compute the aeroelastic responses of general wing-body configurations using the Euler/Navier-Stokes equations for fluids and plate/shell finite-element equations for structures. The coupled equations are solved using a time-integration method with configuration-adaptive moving grids. The results are validated for wings and demonstrated for typical wing-body configurations. Typical aeroelastic responses are computed at transonic Mach numbers.

Governing Aerodynamic Equations

The strong conservation law form of the Navier-Stokes equations is used for shock capturing purposes. The thin-layer version of the equations in generalized coordinates can be written as[13]

$$\partial_\tau \hat{Q} + \partial_\xi \hat{E} + \partial_\eta \hat{F} + \partial_\zeta \hat{G} = Re^{-1} \partial_\zeta \hat{S} \qquad (1)$$

where $\hat{Q}, \hat{E}, \hat{F}, \hat{G}$, and $\hat{S}$, are flux vectors in generalized coordinates. The following transformations are used in deriving Eq. (1).

$$\begin{aligned} \tau &= t \\ \xi &= \xi(x, y, z, t) \\ \eta &= \eta(x, y, z, t) \\ \zeta &= \zeta(x, y, z, t). \end{aligned} \qquad (2)$$

It should be emphasized that the thin-layer approximation is valid only for high Reynolds number flows, and that very large turbulent eddy viscosities invalidate the model.

To solve Eq. (1), ENSAERO has time-accurate methods based on both central-difference and upwind schemes.[14] In this paper, the central-difference scheme based on the implicit approximate factorization algorithm of Beam and Warming[15] with modifications by Pulliam and Chaussee[16] for diagonalization is used. This scheme is first order accurate in time.

For turbulent flow, the coefficient of viscosity needed for Eq. (1) is modeled using the Baldwin-Lomax algebraic eddy-viscosity model.[17] All viscous computations presented in this paper assume fully turbulent flow. This approximation is consistent with the high Reynolds number assumption. For vortex-dominated flow structures of highly swept wings, a modification to the original Baldwin-Lomax model is required. For this study, the Degani-Schiff modification[18] to the original model for treating vortical flows is used.

Aeroelastic Equations of Motion

Following the formulation given in Chapter 20 of Ref. 12, the FE matrix form of the aeroelastic equation of motion is

$$[M]\{\ddot{q}\} + [G]\{\dot{q}\} + [K]\{q\} = \{Z\} \qquad (3)$$

where [M], [G], and [K] are the global mass, damping, and stiffness matrices, respectively. $\{Z\}$ is the aerodynamic force vector corresponding to the nodal displacement vector $\{q\}$.

In this work, it is assumed that the wing-body configuration can be modeled using plate/shell elements. For this purpose, it is further assumed that

the structural properties of the body and wing are represented by equivalent shell and plate elements. The ANS4 shell/plate element is used to represent the structural properties of the wing-body configuration.[19] The ANS4 element shown in Fig. 1 is a 20 degrees-of-freedom (DOF) element which can model both plates and shells. It is based on assumed natural strain approach. For the wing-body configuration considered in this work, the wing and the body are modeled using plate and shell options of the ANS4 element, respectively. At each node, the DOF allowed are the inplane displacements u and v, transverse deflection (w), rotation about x-axis (θ) and rotation about y-axis (ϕ).

The main effort after selecting the FE model of the structure falls into computing the global force vector $\{Z\}$ of Eq. (4). $\{Z\}$ is computed by solving the Euler/Navier-Stokes Eq. (1) at given time, t. First, the pressures are computed at all surface grid points. The forces corresponding to the nodal DOF are computed using the FE nodal fluid-structural interfaces discussed in the next section.

Fluid-Structural Interfaces

In aeroelastic analysis, it is necessary to represent equivalent aerodynamic loads at the structural nodal points and to represent deformed structural configurations at the aerodynamic grid points. In the present domain decomposition approach, coupling between the fluid and structural domains is achieved by combining the boundary data such as aerodynamic pressures and structural deflections at each time step. An analytical moving grid technique has been successfully used to deform the aerodynamic grid according to structural deflections at the end of every time step.[7] There are several different ways to obtain the global force vector $\{Z\}$ of Eq. (3) depending on the equations used for the structural dynamic analysis.

A number of numerical procedures have been developed to exchange the necessary information between the aerodynamic and structural domains.[7] A bi-linear interpolation and a virtual-surface interface are used in this study. The bi-linear interpolation is also called the lumped load (LL) approach. In this approach, the force acting on each element of the structural mesh is first calculated, and then the element nodal force vector is obtained by distributing the total force. The global force vector is obtained by assembling the nodal force vectors of each element. In addition, the deformed configuration of the CFD grid at the surface is obtained by linearly interpolating nodal displacements at finite-element nodes. This approach does not conserve the work done by the aerodynamic forces and needs fine grids for both fluids and structures to give accurate results.

An alternate to the above LL approach is an improved approach based on virtual surface (VS). In this approach, a mapping matrix developed by Appa[20] is selected to accurately exchange data between the fluid and structural interface boundaries. The reason for selecting Appa's method is that the mapping matrix is general enough to accommodate changes in fluid and structural models easily. In addition, this approach conserves the work done by aerodynamic forces when obtaining the global nodal force vector. This method introduces a virtual surface between the CFD surface grid and the finite element mesh for the wing. This virtual surface is discretized by a number of finite elements, which are not necessarily the same elements used in the structural surface modeling.

By forcing the deformed virtual surface to pass through the given data points of the deformed structure, a mapping matrix relating displacements at structural and aerodynamic grid points is derived as

$$[T] = [\psi_a]\left(\delta^{-1}[K] + [\psi_s]^T[\psi_s]\right)^{-1}[\psi_s]^T \qquad (4)$$

where

$[K]$: the free-free stiffness of the virtual surface

ψ_s: displacement mapping from virtual to structural grids

ψ_a: displacement mapping from virtual to aerodynamic grids

δ: penalty parameter

Then, the displacement vector at the aerodynamic grid, $\{q_a\}$, can be expressed in terms of the displacement vector at the structural nodal points, q_s, as

$$\{q_a\} = [T]\{q_s\}.$$

From the principle of virtual work, the nodal force vector, $\{Z_s\}$, can be obtained as

$$\{Z_s\} = [T]^T\{Z_a\}$$

where $\{Z_a\}$ is the force vector at the aerodynamic grids. This procedure is illustrated in Fig. 2.

The aeroelastic equation of motion, Eq. (3), is solved by a numerical integration technique based on the constant-average-acceleration method.

Aeroelastic Configuration Adaptive Grids

One of the major difficulties in using the Euler/Navier-Stokes equations for computational aerodynamics lies in the area of grid generation. For steady flows,

advanced techniques such as blocked zonal grids[1] are currently being used. However, grid-generation techniques for aeroelastic calculations which involve moving components, are still in the early stages of development. In Ref. 7, aeroelastic configuration adaptive dynamic grids were successfully used for computing time-accurate aeroelastic responses of wings using a C-H grid topology.

In this work, an H-O type grid topology is used (H in the streamwise and O in the spanwise directions) for wing-body configuration. This type of grid topology is more suitable for a general wing-body configurations. It gives better surface grid resolution on the body when compared to the C-H grid topology used in Ref. 7. The base surface grid is generated using the S3D code.[21] From the surface grid, the field grid is generated using an analytical approach. In this approach, grid lines in the radial direction away from the surface are generated line by line in the planes normal to the x-axis. The new grid lines are generated in such a way that the radial lines are approximately normal to the previous line. For example, the first line from the surface is generated such that the radial lines are approximately normal to the surface. In this process the spacing between lines are exponentially increased away from the surface. This base grid is used for computing pressures on the rigid configuration. For aeroelastic analysis, the displacements at structural nodes are computed first using Eq. (3). These displacements are then mapped onto the surface grid points by the interface approach discussed above. Finally the field grid is analytically generated starting from the new deformed surface.

Results

Computations on Wing Configuration

To demonstrate aeroelastic computations, a typical fighter type wing of aspect ratio three and taper ratio 1/7 with the NACA 65A006 airfoil section was selected. The sweep angle at the quarter chord line ($\Lambda_{c/4}$) is 45 deg. The transonic flutter characteristics of this wing are available from wind tunnel tests[22] for various flow parameters.

In this computation, the flow field is discretized using a C-H grid topology of size 151 × 30 × 35. The 20 DOF ANS4 shell/plate element[19] was used for the FE modeling of the wing structure. The wing is modeled as a flat plate. Considering the wing structure used in the experiment, variation of mass density is allowed along both chordwise and spanwise directions. However, the thickness of the finite element model is kept constant. This is based on assumptions that the stiffness of the wing is dominated by the aluminum-

alloy insert and the mass distribution of the wing is significantly changed due to plastic foams covering the aluminum-alloy insert. This finite-element plate model predicts natural vibration modes of the wing that compare well with the experiment. The first three modal frequencies computed by using the finite element model are 21.8, 78.1, and 126 Hz and corresponding values measured in the experiment are 21.6, 79.7, and 121 Hz, respectively.

This is the first time a shell/plate FE model has been directly coupled with the Euler/Navier-Stokes equations. As a result, the validity of the coupling approach will be verified by comparing the FE results with those from the previously well-validated modal analysis. In this calculation, the FE computations were made using 36 plate elements and the modal computations were made using the first six modes of the wing. Six elements each were assigned along the chordwise and spanwise directions, respectively. Figure 3 shows the identical displacement responses of the leading edge at the tip obtained by both FE and modal analyses for $M_\infty = 0.854$, p = 0.70 psi and $\alpha = 1.0$ deg. Dynamic aeroelastic computations were made setting a high value for the damping coefficient so that the final results would approach to steady state conditions. The VS approach was used to calculate nodal forces for both FE and modal analysis. Results in Fig. 3 demonstrate the validity of the coupling of plate elements with the Euler/Navier-Stokes equations. The FE approach gives displacements about 0.1 % higher than the modal approach. Such results are expected since the modal approach yields a structure that is stiffer than the actual one, whereas the FE approach represents the actual structural stiffness.

The accuracy of the results can depend on the type of interfaces between fluids and structures. In the following calculations the simple lumped load and the more accurate virtual surface interfaces are compared to each other and the results are shown in Fig. 4. The wing structure was modeled using 100 ANS4 elements. Ten elements each were assigned along the chordwise and spanwise directions, respectively. For a given dynamic pressure of 1.0 psi and initial acceleration of 1.0×10^5 inches/sec, the time history of total lift on the wing is presented in Fig. 4. The total lift obtained by integrating the pressure coefficients at CFD grid points is also shown in the figure. The total lift using CFD grid points is more accurate than those from VS and LL methods. Both VS and LL approaches obtain the total lift by summing the forces at the FE nodal points, which was transformed from the pressure coefficients through interfaces. The VS approach transfers pressure data more accurately than the LL approach. The LL approach shows that the response around peaks

deviates from the CFD solution. For this case the LL approach shows favorable agreement with the VS approach.

Aeroelastic responses were also computed for various dynamic pressures in order to predict flutter dynamic pressure and compared with the experiment.[22] Figure 5 shows the stable, near neutrally stable, and unstable responses of wing tip displacements at the leading edge for dynamic pressures of 0.85, 0.80, and 0.75 psi for $M_\infty = 0.854$. The Navier-Stokes equations and the virtual surface interface are used to obtain the FE nodal force vector. From the responses shown in Fig. 5, the interpolated dynamic pressure for the neutrally stable condition is 0.79 psi. It is noted that the experimental dynamic pressure measured at the neutrally stable condition was 0.91 psi. Considering the lack of experimental pressure data on the wing and the error involved in modeling the wing as a plate with constant thickness, the result is a favorable prediction of the flutter dynamic pressure.

ENSAERO has capability of modeling both the Euler and Navier-Stokes equations. It is of interest to know the effect of the type of flow equations on aeroelastic responses. Such studies will lead to the right choice of methods. For this purpose computations are made at a high-transonic Mach number of 0.970. Figure 6 shows the comparison between the steady pressures obtained from Euler and Navier-Stokes solutions. Since the Mach number is high-transonic, viscous effects are dominant. As a result there are significant differences between the Euler and Navier-Stokes solutions near and behind the shockwave. The Navier-Stokes solutions predict lower negative pressures near the shock waves. The viscous effects on the integrated total lift is shown in Fig. 7. The influence of viscous effects on the aeroelastic responses are shown in Fig. 8. In this case, aeroelastic computations are made when the wing is pitching up to one degree angle of attack (AoA) at a pitch rate of 0.01. Because of the reduced aerodynamic loads, the tip response from the Navier-Stokes solution is lower than that from the Euler solution.

Computations on Wing-Body Configuration

As stated in the introduction one of the main reasons for modeling structures directly by finite elements instead of modes is to extend the fluid/structure interaction computational capability to more complex structures. The procedures demonstrated in the previous section are not limited to simple wing configurations. In this section, results are demonstrated for general wing-body configurations where it is not trivial to pre-select modes.

The selected wing-body configuration shown in Fig. 9 was modeled using a H-O type grid topology using a grid size of 99 x 79 x 30. Earlier work indicated that this grid was adequate for transonic flow computations at moderate angles of attack.[23]

In order to study the effect of structural flexibility on the flow, aeroelastic computations were made for the above wing-body configuration. Both the body and wing are allowed to be flexible. The wing is modeled using 30 plate elements and the body is modeled using 90 shell elements. The FE layout is shown in Fig. 10. Symmetric boundary conditions are applied at the top and bottom body symmetry lines. All DOF are constrained along the wing-body junction. This results in a total of 646 DOF for structures. This FE capability is incorporated in ENSAERO Version 3.1 in a modular way. The skyline data structure is used for the global stiffness and mass matrices.

The structural properties required for the analysis results in frequencies that represent a typical transport type wing-body. Figure 11 shows the mode shapes of the first four modes. For the current structural property assumptions, the first four modes are dominated by wing modes. The present 148-node FE model of the wing-body configuration can compute up to 646 modes.

As stated earlier, an analytical moving grid capability is implemented in ENSAERO based on H-O topology. The grid generated by the code when both the wing and the body are deformed is shown in Fig. 12. It is noted that the singular planes upstream of the leading edge and downstream of the trailing edge are deformed according to the deformed shape of the configuration.

Forced Motion of Flexible Configuration

In order to verify the coupling of the surface movement with the grid movement, computations are made by forcing the motion. Computations are made at $M_\infty = 0.90$, $\alpha = 0.0$ deg and a reduced frequency $k(= \omega c/U)$ equal to 0.50, allowing the configuration to deform in the first torsional mode of the wing. The wing undergoes a torsional mode such that the maximum torsional angle at the tip is 1 deg. The unsteady computations are started from the converged steady state solution and 2400 time steps per cycle of oscillation are required. This corresponds to a nondimensional computational time step size $\Delta\tau = 0.0058$. Figure 13 shows the wing sectional lifts for various sections. As expected, the magnitude of the sectional lift increases towards the tip. A periodic lift response is obtained within two cycles of oscillations.

5

Free Motion on Aeroelastic Configuration

In this section, aeroelastic computations are made on the flexible wing-body configuration by directly coupling the pressures computed solving the Navier-Stokes equations with the FE structural equations. The LL interface is used for this computation. The structural properties of the wing-body configuration are selected to represent a typical aircraft. It is assumed that the wing-root is 256 inches long and aeroelastic computations are made at a dynamic pressure of 1.0 psi.

Demonstration computations are made for a static aeroelastic case when the configuration is ramping up from 0 to 5 deg AoA at $M_\infty = 0.90$. The configuration is pitched up about the axis perpendicular to the wall and located at the leading edge of the wing-root. Starting from the steady state solution the configuration is pitched up at a rate of 0.0012 deg per time step. This pitch rate was adequate to obtain a stable and accurate solution. At every time step the static equilibrium position is obtained by solving the static aeroelastic equations. At the end of each time step a new field grid is generated that conforms to the deformed surface. Figure 14 shows the response of the leading edge of the tip section.

Computational Resources

The current Navier-Stokes version of ENSAERO runs at 380 MFLOPS on the CRAY C90 at Ames Research Center. To run a rigid case, the code requires 33 words of central memory per grid point and 7 microseconds of CPU time per time step per grid point. For the flexible case there is an additional memory requirement of 1000 words per node and CPU time of 25 microseconds per time step per node. A typical dynamic aeroelastic response such as that shown in Fig. 14 requires about 4 CPU hours and 8 million words of central memory.

Discussions and Conclusions

A domain-decomposition computational procedure is developed to compute aeroelastic responses using the Navier-Stokes flow solutions directly coupled with finite-element structural equations. The procedure is demonstrated using plate/shell finite elements. Aeroelastic computations are made for a typical wing-body configuration. Based on this work the following conclusions can be made.

1. It is feasible to directly couple the finite-difference flow equations and finite-element structural equations to obtain accurate results, though each discipline is solved in a separate computational domain. This domain decomposition approach takes advantage of efficient methods developed for each individual discipline.

2. The use of finite-element structures in place of modal structures produces more accurate and detailed results.

3. There is an increase in the requirement of computational time (about 8 %) and memory for FE structures compared to the modal structures (for modal structures memory requirement is negligible).

4. The present domain decomposition approach will be extended for non-linear structures.

5. This approach is suitable for parallel computers. Work is in progress at the Ames Research Center to implement ENSAERO on Intel iPSC/860 parallel computer under NASA's High Performance Computing and Communications (HPCC) Program.

References

[1] Holst, T. L, Flores, J., Kaynak, U., and Chaderjian, N. , "Navier-Stokes Computations, Including a Complete F-16 Aircraft," Chapter 21, Applied Computational Aerodynamics, edited by P. A. Henne, Vol. 125, *Progress in Astronautics and Aeronautics*, AIAA, ISBN 0-930403-69-X, 1990.

[2] Yang, T. Y., *Finite Element Structural Analysis*, Prentice-Hall, Inc., Englewood Cliffs, New Jersey, 1986.

[3] Guruswamy, P. and Yang, T. Y., "Aeroelastic Time Response Analysis of Thin Airfoils by Transonic Code LTRAN2," *Computers and Fluids*, Vol. 9, No. 4, Dec. 1980, pp 409-425.

[4] Borland, C. J. and Rizzetta, D., "XTRAN3S-Transonic Steady and Unsteady Aerodynamics for Aeroelastic Applications, Volume I–Theoretical Manual," AFWAL-TR-80-3107, Dec. 1985.

[5] Guruswamy, G. P., Goorjian, P. M., and Merritt, F. J., "ATRAN3S-An Unsteady Transonic Code for Clean Wings," NASA TM 86783, Dec. 1985.

[6] Batina, J. T., Bennett, R. M., Seidal, D. A., Cunningham, S. R., and Bland, S. R. , "Recent Advances in Transonic Computational Aeroelasticity," NASA TM 100663, Sept. 1988.

[7] Guruswamy, G. P., "Unsteady Aerodynamic and Aeroelastic Calculations of Wings Using Euler Equations," AIAA *Journal*, Vol. 28, No. 3, March 1990, pp 461-469.

[8] Guruswamy, G. P., "Vortical Flow Computations on a Flexible Blended Wing-Body Configuration," AIAA *Journal* , Vol. 30, No. 10, Oct. 1992, pp 2497-2503.

[9] Guruswamy, G. P., "ENSAERO–A Multidisciplinary

Program for Fluid/ Structural Interaction Studies of Aerospace Vehicles," *Computing System Engineering*, Vol. 1, Nos. 2-4, 1990, pp 237-256.

[10] Bendiksen, O. O., "A New Approach to Computational Aeroelasticity," AIAA-91-0939-CP, Baltimore, MD April 1991 pp 1712-1727.

[11] Felker, F. F., "A New Method For Transonic Static Aeroelastic Problems," AIAA-92-2123-CP, Dallas, Texas, April 1992, pp 415-425.

[12] Zienkiewicz, O. C., *The Finite Element Method*, Third Edition, McGraw Hill Book Company (UK) Limited, Maindenhead, Berkeshire, England, 1977.

[13] Peyret, R. and Viviand, H., "Computation of Viscous Compressible Flows Based on Navier-Stokes Equations," AGARD AG-212, 1975.

[14] Obayashi, S, Guruswamy, G. P., and Goorjian, P. M., "Streamwise Upwind Algorithm for Computing Unsteady Transonic Flows Past Oscillating Wings," AIAA *Journal*, Vol. 29, No. 10, Oct. 1991, pp 1668-1677.

[15] Beam, R. and Warming, R. F., "An Implicit Finite-Difference Algorithm for Hyperbolic Systems in Conservation Law Form," *Journal of Computational Physics*, Vol. 22, No. 9, Sept. 1976, pp. 87-110.

[16] Pulliam, T. H., and Chaussee, D. S., "A Diagonal Form of an Implicit Approximate Factorization Algorithm," *Journal of Computational Physics*, Vol. 39, No. 2, Feb. 1981, pp 347-363.

[17] Baldwin, B. S. and Lomax, H. ,"Thin-Layer Approximation and Algebraic Model for Separated Turbulent Flows," AIAA Paper 78-257, Huntsville, Alabama, 1978.

[18] Degani, D. and Schiff, L. B., "Computation of Turbulent Supersonic Flows Around Pointed Bodies Having Cross Flow Separation," *Journal of Computational Physics*, Vol. 66, No. 1, Sept. 1986, pp 173-196.

[19] Park, K. C., Pramono, E. Stanley, G. M. and Cabiness, H. A., "The ANS Shell Elements: Earlier Developments and Recent Improvements, " Analytical and Computational Models of Shells, Edited by Noor, A.K. et al, CED-Vol.3, ASME, New York, 1989, pp 217-240.

[20] Appa, K.,"Finite-Surface Spline, " J. of Aircraft, Vol. 26, No. 5, May 1989, pp. 495-496.

[21] Luh, R. C., Pierce, L. and Yip, D., "Interactive Surface Grid Generation," AIAA Paper 91-0796, Reno Nevada, Jan. 1991.

[22] Dogget, R. V., Rainey, A. G. and Morgan, H. G., "An Experimental Investigation of Aerodynamics Effects of Airfoil Thickness on Transonic Flutter Characteristics, " NASA TM X-79, 1959.

[23] Obayashi, S., Guruswamy, G. P., and Tu, E. L., "Unsteady Navier-Stokes Computations on a Wing-Body Configuration in Ramp Motion," AIAA-91-2865, New Orleans, Louisiana, August 1991.
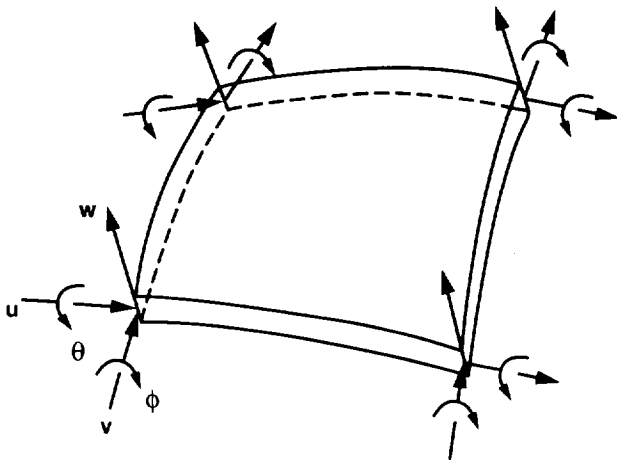
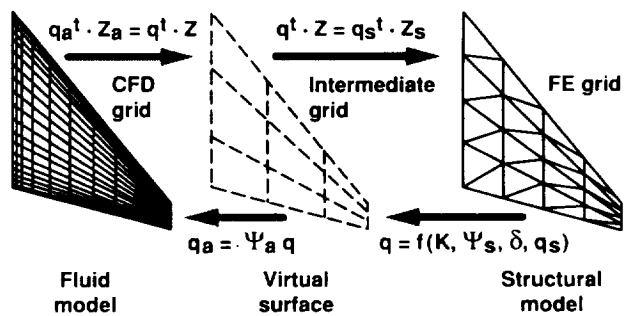Fig. 1 Twenty degrees-of-freedom ANS4 shell/plate finite element.

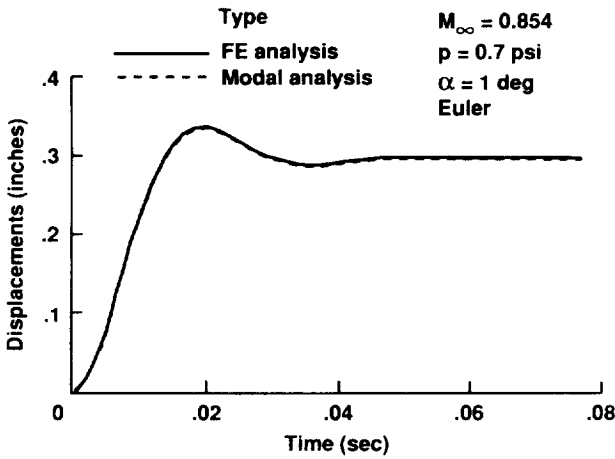Fig. 2 Fluid-structure interfacing using virtual surface approach.

Fig. 3 Validation of finite element implementation in ENSAERO
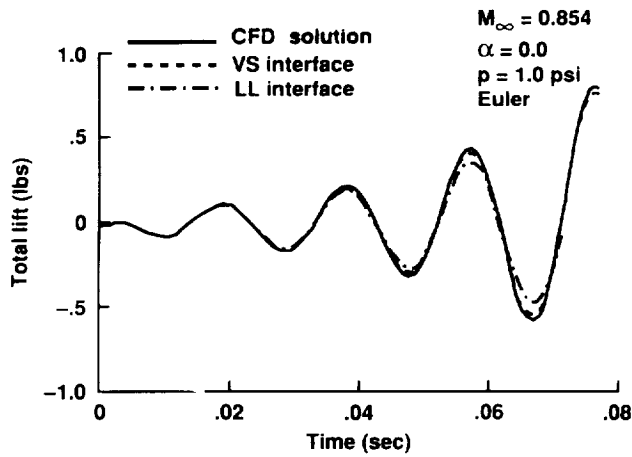

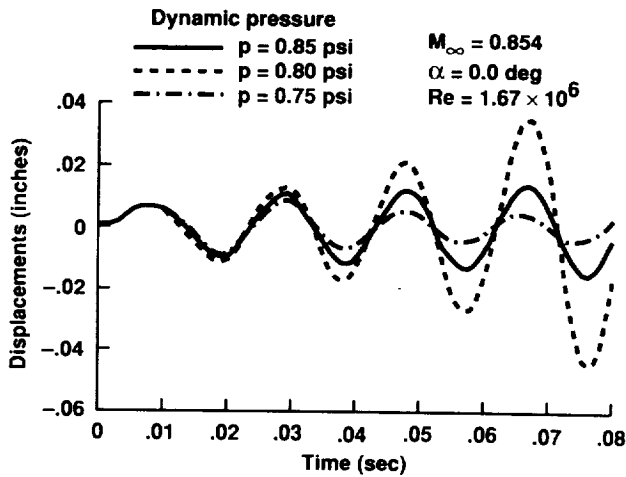Fig. 4 Comparison of lumped load and virtual surface interfacing methods.

Fig. 5 Aeroelastic responses using a finite element model for structures.
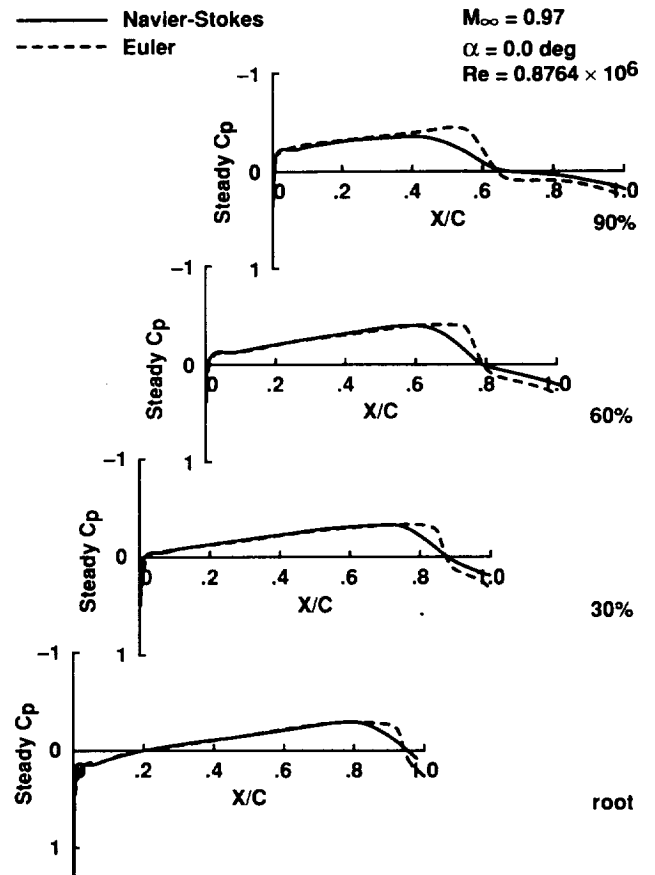

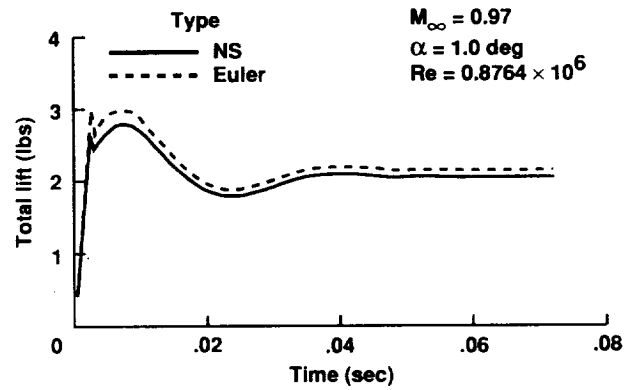Fig. 6 Comparison of transonic steady pressures from Euler and Navier-stokes solutions.

Fig. 7 Comparison of total lift from Euler and Navier-stokes solutions.
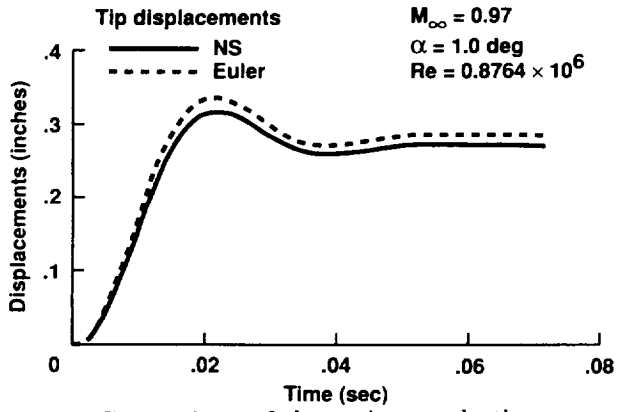
Fig. 8 Comparison of dynamic aeroelastic responses from Euler and Navier-stokes solutions
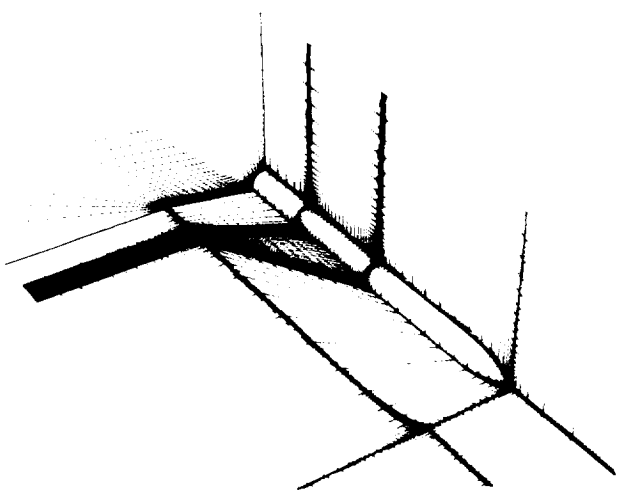

Fig. 11 First four natural modes of the wing-body configuration.

Fig. 9 Typical wing-body configuration with portions of surface and field physical grids.

Total elements = 120
Total nodes = 148
B.C.'s: 1) symmetric conditions
at top and bottom of
the body.
2) fix all DOF's along
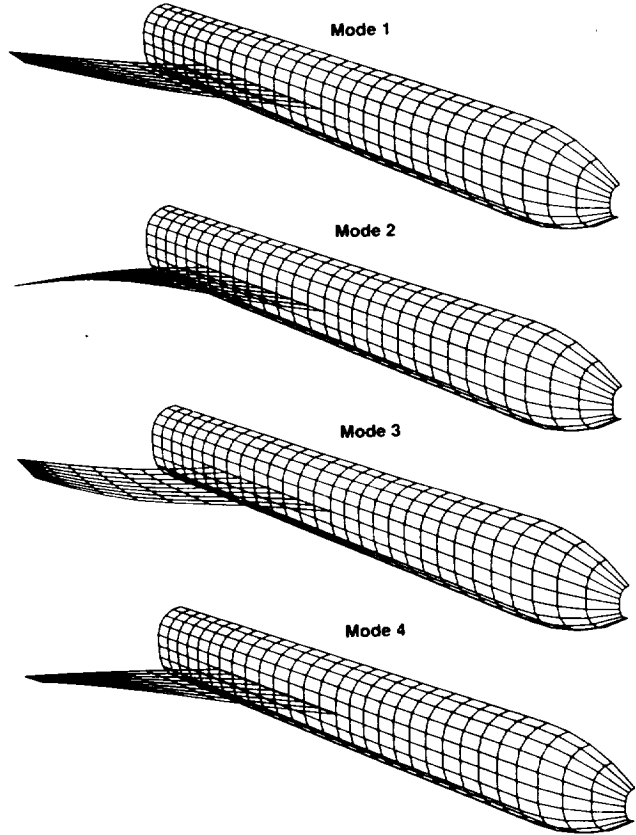wing-body junction.

Total eq'ns: 646

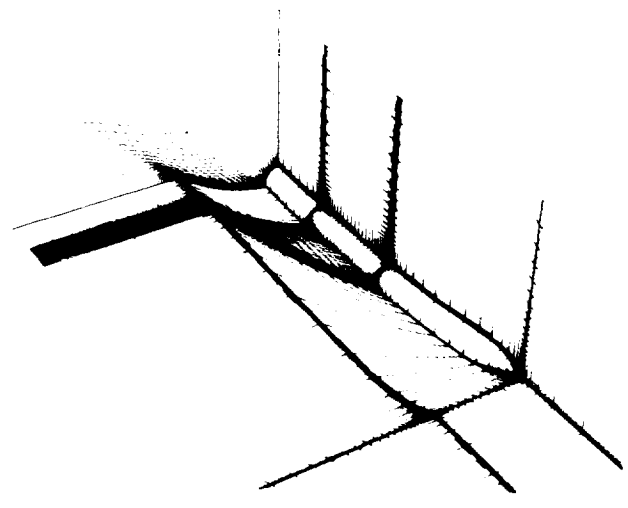Fig. 10 Finite-element modeling of the wing-body configuration.

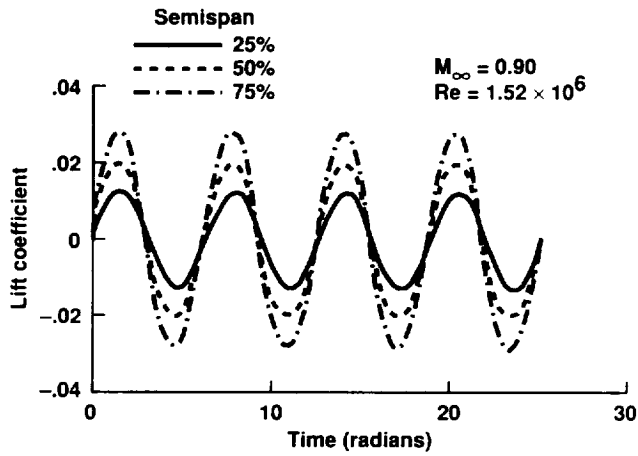Fig. 12 Deformed surface and field grids.

9

Fig. 13 Comparison of sectional lift responses for wing twisting mode.
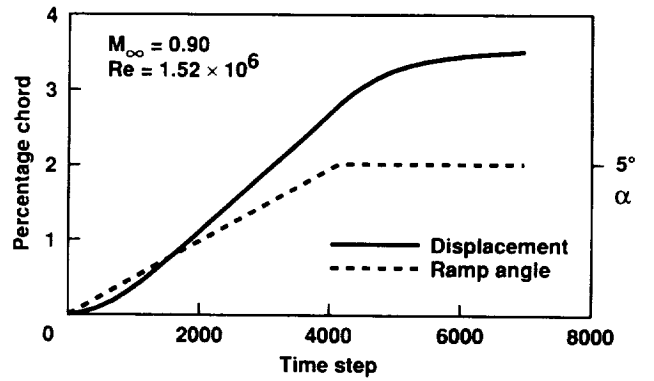
Fig. 14 Static aeroelastic displacements of wing-tip leading edge

APPENDIX B.

A Comparative Study of Serial and Parallel Aeroelastic Computations of Wings

Chansup Byun and Guru P. Guruswamy

January 1994

NASA
National Aeronautics and
Space Administration

A Comparative Study of Serial and Parallel Aeroelastic Computations of Wings

Chansup Byun and Guru P. Guruswamy

NASA

A COMPARATIVE STUDY OF SERIAL AND PARALLEL AEROELASTIC COMPUTATIONS OF WINGS

Chansup Byun* and Guru P. Guruswamy
Ames Research Center

SUMMARY

This paper presents a procedure for computing the aeroelasticity of wings on parallel multiple-instruction, multiple-data (MIMD) computers. In this procedure, fluids are modeled using Euler equations, and structures are modeled using modal or finite element equations. The procedure is designed in such a way that each discipline can be developed and maintained independently by using a domain decomposition approach. In the present parallel procedure, each computational domain is scalable. A parallel integration scheme is used to compute aeroelastic responses by solving fluid and structural equations concurrently. The computational efficiency issues of parallel integration of both fluid and structural equations are investigated in detail. This approach, which reduces the total computational time by a factor of almost 2, is demonstrated for a typical aeroelastic wing by using various numbers of processors on the Intel iPSC/860.

INTRODUCTION

In recent years, significant advances have been made for single-discipline use of both computational fluid dynamics (CFD), using finite-difference approaches, and computational structural dynamics (CSD), using finite-element methods. In single disciplines, computations have been made on complete aircraft. However, only a limited amount of work has been completed in coupling these two disciplines for multidisciplinary applications. The prime reason is the lack of computational power for combining the two major computational fields. The development of a new generation of parallel computers can possibly alleviate the restriction of computational power.

A multidisciplinary code for computing unsteady flows and aeroelastic responses of aerospace vehicles, ENSAERO, has been developed on serial supercomputers at the Computational Aerosciences Branch of the NASA Ames Research Center (ref. 1). This multidisciplinary code computes unsteady aerodynamic responses of aircraft using the Euler/Navier-Stokes equations. The modal or finite element equations are used to model structures. An aeroelastic shape-conforming moving grid is used to include the effect of structural deformations on unsteady flows. This code is designed in a modular fashion to adopt several different numerical schemes suitable for accurate aeroelastic computations. The basic coding

---

*MCAT Institute.

of ENSAERO can accommodate zonal grid techniques for efficient modeling of full aircraft.

An early version of ENSAERO (ref. 2) has been successfully applied in computing aeroelastic responses of a rectangular wing by using the Euler equations for fluids and the modal equations for structures. The result demonstrates that the code can accurately predict the flutter dynamic pressure of a rectangular wing. The code was extended to compute aeroelastic responses using the Navier-Stokes equations for fluids (ref. 3). Later, it was updated by utilizing an upwind algorithm, and the code has been applied to fighter wings undergoing unsteady motions (refs. 4 and 5) at moderately large angles of attack. This code also has a capability of modeling moving control surfaces (ref. 6). Furthermore, ENSAERO has demonstrated the capability to simulate transonic flows on wing-body configurations using the Navier-Stokes equations (ref. 7).

For simple geometries such as clean wings, the modal approach can produce accurate response results. However, the modal approach may be less accurate for complex structures such as wing-body configurations. In order to accurately represent aeroelastic responses of general wing-body configurations, the finite element equations for structures have been implemented in ENSAERO. A typical wing-body configuration has been used to demonstrate aeroelastic responses at transonic Mach numbers using the Navier-Stokes equations for fluids and the finite element equations for structures (ref. 8). Two-noded beam elements are used to model the wing-body structures. Each node has three degrees of freedom (DOF) corresponding to transverse displacement and to transverse and torsional rotations, respectively.

In the past, all computations were accomplished serially, on computers such as the Cray Y-MP at Ames Research Center. Currently, a version of ENSAERO (ref. 9) that uses the Euler equations for fluids and the modal equations for structures has been parallelized on the Intel iPSC/860 at Ames. The Intel iPSC/860 is a distributed-memory, multiple-instruction, multiple-data (MIMD) computer with 128 processors. In this parallel implementation, a domain decomposition approach is used in which the fluid equations and the structural equations are modeled in separate computational domains. Each domain is mapped individually onto a group of processors, referred to as a cube on the Intel iPSC/860. As a result, each discipline can be developed and implemented independently of the others. However, because of the coupling between the disciplines, there is a need to exchange data, such as pressures and structural deformations at interfaces. This exchange between the fluid and structural domains is accomplished through an intercube communication mechanism (ref. 10), which enables different processors in each cube to communicate directly.

In this work, procedures to compute aeroelastic responses on MIMD parallel computers using direct coupling of the Euler equations for fluids and the modal or finite element equations for structures are investigated for wings. The implementation of the structural domain on the iPSC/860 is described in detail. In addition, the computational efficiency issues of parallel integration of both fluid and structural

equations are investigated in detail. The proposed integration scheme exploits the architecture of MIMD computers. This research will provide an efficient procedure for aeroelastic analysis on MIMD computers.

GOVERNING AERODYNAMIC EQUATIONS

The strong conservation-law form of the Euler equations is used for shock-capturing purposes. The Euler equations in generalized coordinates can be written as (ref. 11)

$$\partial_\tau \hat{Q} + \partial_\xi \hat{E} + \partial_\eta \hat{F} + \partial_\zeta \hat{G} = 0 \tag{1}$$

where $\hat{Q}$, $\hat{E}$, $\hat{F}$, and $\hat{G}$ are flux vectors in generalized coordinates. The following transformations are used in deriving equation (1):

$$\begin{aligned}
\tau &= t \\
\xi &= \xi(x, y, z, t) \\
\eta &= \eta(x, y, z, t) \\
\zeta &= \zeta(x, y, z, t)
\end{aligned} \tag{2}$$

To solve equation (1), ENSAERO has time-accurate methods based on both central-difference and upwind schemes (ref. 12). In this work, the central-difference scheme based on the implicit approximate factorization algorithm of Beam and Warming (ref. 13) with modifications by Pulliam and Chaussee (ref. 14) for diagonalization was used. This scheme is first order accurate in time.

AEROELASTIC EQUATIONS OF MOTION

The governing aeroelastic equations of motion for structures can be written as

$$[M]\{\ddot{q}\} + [C]\{\dot{q}\} + [K]\{q\} = \{Z\} \tag{3}$$

where $[M]$, $[C]$, and $[K]$ are the global mass, damping, and stiffness matrices, respectively, and where $\{Z\}$ is the aerodynamic force vector corresponding to the displacement vector $\{q\}$. These quantities can be expressed in modal coordinates or finite element coordinates depending on the method used to obtain structural dynamic responses. One of the main efforts is concerned with the computation of the global force vector $\{Z\}$ of equation (3). In this work, for a given time t, $\{Z\}$ is computed by solving the Euler equations. From the solution of equation (1), pressure coefficients are computed at all grid points on the wing surface. Using

3

these pressure coefficients, the force vector $\{Z\}$ is calculated by means of the modal matrix or a fluid-structural interface, which is described in the next section.

The aeroelastic equations of motion (3) have been solved in past work (refs. 2 and 8) by a numerical integration technique based on the linear acceleration method (ref. 15). This method has been successfully used for integrating the modal equations, assuming a linear variation of the acceleration. However, this integration method requires a very small time step in order to integrate the finite element equations of motion. As a result, for the finite element equations of motion, the constant-average-acceleration method (ref. 16) is adopted to increase the time-step size. This method is an extension of the linear acceleration method. Assuming a constant average acceleration on a time interval, the velocities and displacements are obtained at a time t as

$$
\begin{aligned}
\{\dot{q}\}_t &= \{\dot{q}\}_{t-\Delta t} + \frac{\Delta t}{2}\{\ddot{q}\}_{t-\Delta t} + \frac{\Delta t}{2}\{\ddot{q}\}_t \\
\{q\}_t &= \{q\}_{t-\Delta t} + \Delta t\{\dot{q}\}_{t-\Delta t} + \frac{\Delta t^2}{4}(\{\ddot{q}\}_t + \{\ddot{q}\}_{t-\Delta t})
\end{aligned}
\tag{4}
$$

Using these equations, the displacements at the end of a time interval can be obtained by solving

$$
[D]\{q\}_t = \{Z\}_t + [M]\{a\} + [C]\{v\} \tag{5}
$$

where

$$
[D] = [K] + \frac{4}{\Delta t^2}[M] + \frac{4}{\Delta t}[C]
$$

$$
\{a\} = \frac{4}{\Delta t^2}\{q\}_{t-\Delta t} + \frac{4}{\Delta t}\{\dot{q}\}_{t-\Delta t} + \{\ddot{q}\}_{t-\Delta t}
$$

$$
\{v\} = \frac{2}{\Delta t}\{q\}_{t-\Delta t} + \{\dot{q}\}_{t-\Delta t}
$$

This is an unconditionally stable scheme, whereas the linear acceleration method is conditionally stable.

FLUID-STRUCTURAL INTERFACES

In aeroelastic analysis, it is necessary to represent the equivalent aerodynamic loads at the structural nodal points and to represent the deformed structural configurations at the aerodynamic grid points. In the present domain decomposition approach, coupling between the fluid and structural domains is achieved by interfacing the boundary data, such as aerodynamic pressures and structural deflections, at each time step. An analytical moving-grid technique has been successfully used to deform the aerodynamic grid according to the structural deflections at the end of every time step (refs. 1, 2, and 8) There are different approaches for obtaining the global force vector $\{Z\}$ of equation (3), depending on the equations used for the structural dynamic analysis.

4

For the modal equations of motion, the global force vector can be easily obtained in terms of the preselected mode shapes (modal matrix) as

$$\{Z\} = \frac{1}{2}\rho U_\infty^2 [\Phi]^T [A] \{\Delta C_p\} \tag{6}$$

where $[\Phi]$ is the modal matrix and $[A]$ the diagonal area matrix of the aerodynamic control points. The unsteady differential pressure coefficients on the wing surface are defined as $\{\Delta C_p\}$. It is noted that the modal matrix is also used to represent the deformation of the wing.

Solution of the equations of motion based on the finite element discretization requires a fluid-structural interface similar to the modal matrix. Several numerical procedures have been developed for exchanging the necessary information between the fluid and structural domains (refs. 17–19). However, in this study, a linear interpolation scheme is first developed for the interface so that coupling of fluid and structural equations could be simple for implementation on the new parallel computers. This scheme is called the lumped load interface. In this method, the force acting on each element of the structural mesh is first calculated and then the element nodal force vector is obtained by distributing the force. The global force vector is obtained by assembling the nodal force vectors of each element. In addition, the deformed configuration of the CFD grid at the surface is obtained by linearly interpolating nodal displacements at finite element nodes.

Next, a mapping matrix developed by Appa (ref. 18) is selected to accurately exchange data between the fluid and structural interface boundaries. The reason for selecting Appa's method is that the mapping matrix is general enough to accommodate changes in fluid and structural models easily. In addition, this approach conserves the work done by aerodynamic forces when obtaining the global nodal force vector. This method introduces a virtual surface between the CFD surface grid and the finite element mesh for the wing. The virtual surface is discretized by a number of finite elements, which are not necessarily the same elements used in the structural surface modeling. This method is called the virtual surface interface.

By forcing the deformed virtual surface to pass through the given data points of the deformed structure, a mapping matrix relating displacements at structural and aerodynamic grid points is derived as

$$[T] = [\psi_a] \left(\delta^{-1}[K] + [\psi_s]^T [\psi_s] \right)^{-1} [\psi_s]^T \tag{7}$$

where

$\quad$ $[K]$ is the free-free stiffness of the virtual surface

$\quad$ ψ_s is the displacement mapping from virtual to structural grids

$\quad$ ψ_a is the displacement mapping from virtual to aerodynamic grids

$\quad$ δ is the penalty parameter

5

Then, the displacement vector at the aerodynamic grid $\{q_a\}$ can be expressed in terms of the displacement vector at the structural nodal points q_s as

$$\{q_a\} = [T] \{q_s\}$$

From the principle of virtual work, the nodal force vector $\{Z_s\}$ can be obtained as

$$\{Z_s\} = [T]^T \{Z_a\}$$

where $\{Z_a\}$ is the force vector at the aerodynamic grids (ref. 20).

PARALLEL IMPLEMENTATION OF THE AEROELASTIC EQUATIONS

The domain decomposition approach used in this study enables data structures and solution methods for fluid and structural equations to be developed independently. Fluid and structural equations are modeled in separate computational domains. However, coupling of the disciplines requires the exchange of the interface boundary data, which is accomplished through an intercube communication mechanism (ref. 10). This intercube communication facility enables different processors in each cube to communicate directly on the iPSC/860. It is important to keep the specification of data exchange routine the same on both computational domains.

The domain for fluids is capable of solving the Euler equations using 3-D uni-partitioning of the computational domain. The uni-partitioning scheme denotes that one grid subdomain is assigned to each of the processors. The arrangement of processors is described in figure 1. The arrows denote bi-directional data communication. There are a variety of concurrent algorithms available for solving the system of equations for fluids. Currently, the solver for the fluid equations can use three different concurrent algorithms: (1) complete exchange-based implementations (CE-GE), (2) pipelined-Gaussian elimination (PGE), and (3) substructured Gaussian elimination followed by solution of the reduced system by means of balanced odd-even cyclic reduction (SGE-BCR) (ref. 21). In this work, the one-way PGE scheme is used. The choice of algorithms was made largely on the basis of memory use. The one-way PGE method allows the use of larger computational grids, or of fewer processors, than do the other schemes. More details about the implementation of the fluid domain can be found in reference 21.

For the structural domain, modal equations were first used on the iPSC/860. Since a limited number of preselected mode shapes were used, only a single processor was assigned to the structural domain. However, in replacing modal equations with the finite element equations, it is necessary to use a cube of multiple processors for structures. In this study, it is assumed that each subdomain of the entire structure is mapped onto a single processor. Each processor stores only the information relevant to the subdomain assigned to it. The information can be the stiffness and

mass matrices and the applied nodal force vector of a subdomain. Then equation (5) is expressed at the subdomain level.

In this work, a regular finite element mesh is used to model wings as a plate, and the domain decomposition is made by using 2-D uni-partitioning as shown in figure 1. This type of domain decomposition enables an efficient and simple message communication mechanism within the structural domain. Only chordwise and spanwise bi-directional messages are exchanged along the subdomain interfaces in the structural domain.

At present, the solver for the structural domain is based on a Jacobi-preconditioned conjugate gradient (JPCG) algorithm on the Intel iPSC/860. The present JPCG algorithm is based on a parallel conjugate gradient algorithm proposed by Law (ref. 22). The algorithm is described in the appendix for completeness. The advantage of Law's algorithm is that it does not form the global system matrices. In this method, the multiplication of a matrix by a trial vector, which is the major operation of the conjugate gradient algorithm, is performed at the subdomain level. The interprocessor communication is confined to the solution phase.

INTEGRATION SCHEMES FOR COUPLED DOMAINS

In a serial computer, the integrations of both fluid and structural equations are performed one after the other in a sequential nature. Figure 2(a) shows the sequential integration scheme implemented on MIMD computers. In the sequential integration scheme, the fluid domain has to wait to proceed to the next time step until it receives information about structural deformations. The structural domain also has to wait for surface pressure data, so both cubes have their own idle times while they wait for data communications. However, since the size of the structural equations was small for modal analysis, the effect of the waiting time was negligible relative to the computational time per integration step.

On the contrary, if a large number of modes or direct finite element equations are used in order to accurately predict dynamic responses of complex structures, the computational time per integration step may be increased rapidly. This is due to the increase in the idle time when a sequential integration scheme is used on the iPSC/860. However, this situation can be avoided by executing the integration of both fluid and structural equations concurrently as shown in figure 2(b). In the proposed parallel integration scheme, both solvers start computations independently and one of the solvers waits until the other finishes its calculation. Then they exchange the required data with each other for the next time step. By doing so, the parallel integration can reduce the idle time since only one cube may have partial idle time. The resulting speedup achieved by the parallel integration scheme is theoretically by a factor of almost 2, provided that computational times required for the fluid and structural domains are well balanced.

7

COMPUTATIONAL RESULTS

To demonstrate an aeroelastic computation, a clipped delta wing of aspect ratio 3 and taper ratio 1/7 with the NACA 65A006 airfoil section was selected. The sweep angle at the quarter chord line $(\Lambda_{c/4})$ is 45°. The transonic flutter characteristics of this wing are available from wind tunnel tests (ref. 23) for various flow parameters.

In this computation, the flow field is discretized by using a C-H grid topology of size $151 \times 30 \times 25$. The CFD grid at the root and the upper surface of the wing is shown in figure 3. The CFD grid is assigned to 32 processors on the iPSC/860. The processors are arranged as a three-dimensional mesh of eight processors in the chordwise direction and two processors in each of the spanwise and surface-normal directions. This same arrangement for fluids is kept throughout the computations so that the performance of the structural domain can be studied in detail.

A 20-DOF ANS4 shell element (ref. 24) was used for the finite element modeling of the wing structure. The wing is modeled as a plate. Considering the wing structure used in the experiment, variation of mass density is allowed along the chordwise and spanwise directions. But the thickness of the finite element model is kept constant. This is based on assumptions that the stiffness of the wing is dominated by the aluminum-alloy insert and that mass distribution of the wing is significantly changed as a result of plastic foams covering the aluminum-alloy insert. This finite element plate model predicts natural vibration modes of the wing that compare well with the experiment. The first three modal frequencies computed by using the finite element model are 21.8, 78.1, and 126 Hz, and corresponding values measured in the experiment are 21.6, 79.7, and 121 Hz, respectively.

Modal Analysis

The first parallel version of ENSAERO was capable of using the Euler equations for fluids and the modal equations for structures. Using this version of ENSAERO, aeroelastic responses were computed. In figure 4, the computed generalized displacements of the first three modes for the wing are presented. The results were obtained for a freestream Mach number (M_∞) of 0.854 and a given dynamic pressure (P) of 0.7 psi. In this calculation, the first six mode shapes of the wing were used to predict the structural dynamic responses. Identical results were obtained from serial and parallel computers. At this point, it is verified that the fluid and structural domains of the parallel ENSAERO and of the intercube communication mechanism are properly working. It should be noted that only one processor is assigned for the structural analysis since only six mode shapes are used to represent the structural properties of the wing. The wall-clock times required for each integration step on a single processor of the Cray Y-MP and on the Intel iPSC/860 are 1.36 and 3.03 seconds, respectively.

8

The proposed parallel integration scheme is compared with the sequential integration scheme used on serial computers. Using both sequential and parallel integration schemes, aeroelastic responses of the wing were computed on the iPSC/860. Aeroelastic responses were computed by simulating experimental conditions for a freestream Mach number of 0.977 and for a given dynamic pressure of 0.65 psi. Results from sequential and parallel integration schemes agree well, as shown in figure 5. Since only six modes were used for the modal analysis, the reduction in computational time was marginal (less than 2% of the time per integration step used in the sequential integration scheme). By increasing the number of modes to 50, the sequential integration scheme required 5% more computational time per integration step whereas the time for the parallel integration scheme remained the same. This trend is more evident as the number of equations increases.

Finite Element Analysis

For simple geometries such as rectangular wings, the modal analysis can accuratly predict dynamic responses. However, the modal analysis with a limited number of preselected mode shapes may be less accurate for complex structures such as wing-body configurations. In order to accurately represent aeroelastic responses of general aircraft configurations, the modal analysis was replaced with the direct finite element analysis in ENSAERO. The finite element equations were first tested on the Cray Y-MP version of the code and then were parallelized on the Intel iPSC/860.

The lumped load and virtual surface interfaces on the Y-MP are shown in figures 6 and 7. The wing structure was modeled using 100 ANS4 elements. Ten elements each were assigned along the chordwise and spanwise directions, respectively. The time history of total lift on the wing for a given dynamic pressure of 1.0 psi and initial acceleration of 1.0×10^5 inches/sec^2, is presented in figure 6. The exact solution is the total lift obtained by integrating pressure coefficients at CFD grid points. Both virtual surface (VS) and lumped load (LL) interfaces obtain the total lift by summing the forces at the finite element (FE) nodal points, which were transformed from pressure coefficients through interfaces. The virtual surface interface transfers pressure data more accurately than the lumped load interface. The lumped load interface shows a favorable result although the response around peaks deviates from the exact solution. In addition, the tip displacements of the wing at the leading edge are presented in figure 7. The lumped load approach shows favorable agreement with the virtual surface approach.

The lumped load approach was first used as the fluid-structural interface for the finite element equations on the iPSC/860. The choice of interfaces was made largely on the basis of memory use. The size of the mapping matrix for the virtual surface interface becomes too large to fit on a single processor on the iPSC/860 when the number of fluid grid points or structural nodal points on the wing increases. However, the lumped load approach requires only a small amount of memory to identify the location of fluid grid points on a finite element discretization.

9

In order to check the parallel implementation of the finite element equations, the tip displacements of the wing were computed, without aerodynamic forces, on the Y-MP and the iPSC/860. This wing was modeled using 64 ANS4 elements. For this computation, processors were assigned as a 2-D mesh of two processors in the chordwise and spanwise directions, respectively, on the iPSC/860. Identical results were obtained on both the Y-MP and the iPSC/860.

For the structural model using finite element equations, the aeroelastic responses were obtained using both sequential and parallel integration schemes on the iPSC/860. The results are presented in figure 8. The responses were obtained for a given dynamic pressure of 1.0 psi. The same finite element mesh and processor arrangement used in the previous case are used for this computation. The two results agree well. The wall-clock times per integration step achieved are 3.45 and 3.00 seconds by using sequential and parallel integration schemes, respectively. The speedup is still marginal since the total number of equations is relatively small (360 DOF) for the structural dynamic analysis. However, for 256 finite elements (1360 DOF) with four processors on the structural domain, the wall-clock times per integration step are 6.22 and 3.33 seconds by using sequential and parallel integration schemes, respectively. The speedup achieved is 1.87 by using the parallel integration scheme. When the computational time between the fluid and structural domains is balanced, maximum speedup can be achieved.

The parallel integration scheme enables the combination of advanced CFD and CSD technologies with minimal increase in the computational time per integration step. The required computational time per integration step is determined by both the fluid and structural domains on serial computers. However, using the parallel integration scheme on MIMD computers, the time is solely determined by the computational domain that requires more time per integration step. This parallel integration is one of the advantages of using MIMD computers for multidisciplinary analysis.

Aeroelastic responses were also computed for various dynamic pressures in order to predict the flutter dynamic pressure. Figure 9 shows the stable, near neutrally stable, and unstable responses of wing tip displacements at the leading edge for dynamic pressures of 0.80, 0.85, and 0.90 psi, respectively. From the responses shown in figure 9, the interpolated dynamic pressure for the neutrally stable condition is 0.84 psi. It is noted that the experimental dynamic pressure measured at the neutrally stable condition was 0.91 psi. Considering the lack of experimental pressure data on the wing and the error involved in modeling the wing as a plate with constant thickness, the computational result is an acceptable prediction of the flutter dynamic pressure.

Performance

In order to support multidisciplinary analysis with practical computational turnaround times for design work, the computational domain on parallel machines must be scalable. This section describes several aspects of performance, including

single processor computational rates, domain decomposition strategy, and scalability of the structural domain in ENSAERO on the iPSC/860. It is noted that only a linear model is used for the dynamic analysis of the structural domain. The performance of the fluid domain can be found in reference 21. All performance data reported are for 64-bit arithmetic.

In order to measure the performance of the structural domain on the Intel iPSC/860, the identical code, except message passing routines, was run on the Y-MP and the averaged time per integration step was obtained. All FLOP rates quoted are calculated by comparing the time per integration step on the iPSC/860 with that on the Y-MP using a single processor. Operation counts from the Cray Hardware Performance Monitor are used.

A single processor of the iPSC/860 was able to house 256 ANS4 elements. The Y-MP equivalent MFLOPS obtained is about 4.2 MFLOPS for this size of problem, and the corresponding rate is about 77 MFLOPS on a single Y-MP processor. This rate is about 7% of the peak performance of a single processor on the iPSC/860. Similar performance was reported by Ryan and Weeratunga for the fluid domain (ref. 21).

The performance of the structural domain in parallel ENSAERO has been measured over a wide range of processor numbers and problem sizes as shown in figure 10. The speedup relative to the Y-MP is defined as

$$speedup = \frac{t_{Cray}}{t_{Intel}}$$

where t_{Cray} and t_{Intel} are the computational time per integration step measured on the Y-MP and the iPSC/860, respectively. Only a single processor is used to measure t_{Cray} on the Y-MP. The open and filled symbols denote the domain decomposition which results in the minimum and maximum bandwidths of the stiffness matrix of each subdomain for a given number of processors.

For the case of 1,360 DOF, the computational time per integration step on the iPSC/860 is barely closed to that on the Y-MP when 64 processors are in use. However, as increasing the size of problem (10,560 and 20,800 DOF), the iPSC/860 achieves about the speed of the Y-MP by using 16 processors. It is evident that the JPCG solver on the iPSC/860 performs better as the size of problem increases. For the case of 20,800 DOF, the relative speedup achieved is about 8 by the time 64 processors are in use.

For a given number of processor, the obtained speedup varies depending on the domain decomposition strategy as shown in figure 10. Only the results for the minimum and maximum bandwidths are presented for clarity. The speedup increases as decreasing the matrix bandwidth of each subdomain for a given number of processors on the iPSC/860. This is due to the fact that the conjugate gradient algorithm is subjected to the multiplication of the coefficient matrix and a trial vector. Since the multiplication is performed only at the subdomain level in the JPCG

solver, the smaller bandwidth results in fewer operations and quicker computational time.

The overall performance of ENSAERO on both the Y-MP and the iPSC/860 is shown in figure 11 for the case of 113,250 grid points for the fluids and 10,560 DOF for the structure. In this computation, 32 processors are assigned to the fluid domain and 16 to 64 processors to the structural domain. Both the skyline reduction and JPCG solvers are compared on the Y-MP but only the JPCG solver is used for the structural domain on the iPSC/860 at the present time. A parallel version of the skyline reduction solver is under implementation.

The height of each column is the time per integration step. Each column is divided into zones representing the time spent for the fluid domain, the structural domain, and for idle/intercube communication. It should be noted that the time per integration step for the skyline reduction solver included only time spent for forward reduction and back substitution without the factorization time. The reason is that the contribution of the factorization time to the computation time per integration step is negligible when a large number of time steps are required to obtain linear dynamic responses. Providing that 7,000 steps are required for a typical aeroelastic computation of the given wing, the increase of the time per integration step is about 0.5% of the time used for structure.

It is evident that the skyline reduction solver outperforms the JPCG solver on the Y-MP. However, the JPCG solver is first implemented on the iPSC/860. The reason is that it is desirable to compare the performance of the two solvers on the iPSC/860. The JPCG solver on the iPSC/860 could not achieve the performance of the skyline reduction solver without including the factorization time on the Y-MP. However, as far as the JPCG solver is concerned, 16 processors on the iPSC/860 can obtain the performance of a single processor on the Y-MP. In addition, the overall performance of ENSAERO using 96 processors on the iPSC/860 is about one-third of that obtained using the skyline reduction solver with a single processor on the Y-MP. This result is based on the averaged time per integration step. It should be noted that the structural domain determined the time per integration step for this particular problem on the iPSC/860. Most of the time on the fluid domain was spent waiting for the interface boundary data. This means that fewer processors can be assigned to the fluid domain without sacrificing computational performance as long as the memory on each processor can accommodate the assigned grid partitioning.

CONCLUSIONS

A parallel version of a multidisciplinary code, ENSAERO, was developed on the Intel iPSC/860. A domain decomposition approach was used to enable the fluid and structural domains to be developed and maintained independently. This approach provides an efficient and effective environment to researchers. A researcher concerned with the fluid or the structural domain can develop his own discipline independent of the others. The only thing to be done together is coupling

of the disciplines. Since coupling of the disciplines is achieved by an intercube communication mechanism, coupling should not cause any problem as long as each domain maintains the specification for intercube communication. This makes it easy for each discipline to incorporate and develop new algorithms or data structures without interferences.

In addition to the modal analysis, the capability of finite element analysis for structural dynamic analysis has been added to parallel ENSAERO. The structural domain on the iPSC/860 is again divided into a number of subdomains. The solution of the structural domain is obtained by the Jacobi preconditioned conjugate gradient (JPCG) solver. The partition of the structural domain for a wing is two-dimensional uni-partitioning since the wing is modeled as a plate and the discretization is a regular mesh. This enables the message communication within the structural domain to be very simple and efficient.

As far as the structural domain is concerned, the performance on the iPSC/860 is still far behind the best performance of the Y-MP a result of the poor performance of the JPCG algorithm. A parallel version of the skyline reduction solver is being implemented for the structural domain on the iPSC/860. This will provide increased performance for the structural domain on the iPSC/860. For a problem size of 10,560 DOF, the overall performance of parallel ENSAERO using 96 processors on the iPSC/860 is about one-third of that obtained using the skyline reduction solver for the structural domain on a single Y-MP processor.

The parallel integration scheme enables the combination of advanced CFD and CSD technologies with minimal increase in computational time per integration step. The computational time per integration step is solely determined by the domain that requires more computational time on the iPSC/860 whereas that time it is determined by both domains on serial computers. This parallel integration is one of the advantages of using MIMD computers for multidisciplinary analysis. The procedure developed in this research will provide an efficient tool for solving aeroelastic problems of complete aerospace vehicle configurations on MIMD computers.

13

APPENDIX

1. Set diagonal elements of global stiffness matrix

    Send $\{K_{j,j}^e\}$ to neighboring processors

    Receive $\{K_{j,j}^i\}$ from neighboring processors

    $\{d^e\} = \Sigma \{K_{j,j}^i\} + \{K_{j,j}^e\}$

2. Set initial trial and residual vectors

    $\{q^e\} = 0$

    $\{r^e\} = \{z^e\}$

3. Set initial search direction

    Send $\{r^e\}$ to neighboring processors

    Receive $\{r^e\}$ from neighboring processors

    $\{s^e\} = \Sigma\{r^i\} + \{r^e\}$

    $z_j^e = s_j^e/d_j^e, \quad j = 1, ..., neq^e$

    $\rho^e = \{r^e\}^T\{z^e\}$

    $\gamma_0 = \Sigma \rho^e, \quad e = 1, ..., np$ (global sum)

    $\gamma = \gamma_0$

    $\{p^e\} = \{s^e\}$

4. Operations at subdomain level

    $\{u^e\} = [K^e]\{p^e\}$

    $\beta^e = \{p^e\}^T\{u^e\}$

    $\sigma^e = \beta^e/\gamma$

5. Update solution and residual

    $1/\alpha = \Sigma \sigma^e, \quad e = 1, ..., np$ (global sum)

    $\{q^e\} = \{q^e\} + \alpha\{p^e\}$

    $\{r^e\} = \{r^e\} - \alpha\{u^e\}$

6. Update search direction and check convergence

    Send $\{r^e\}$ to neighboring processors

    Receive $\{r^e\}$ from neighboring processors

    $\{s^e\} = \Sigma\{r^i\} + \{r^e\}$

    $z_j^e = s_j^e/d_j^e, \quad j = 1, ..., neq^e$

    $\rho^e = \{r^e\}^T\{z^e\}$

    $\gamma_{new} = \Sigma \rho^e, \quad e = 1, ..., np$ (global sum)

    $IF(\gamma_{new}/\gamma_0 < TOLERANCE) \ STOP$

    $\{p^e\} = \{s^e\} + (\gamma_{new}/\gamma) \{p^e\}$

    $\gamma = \gamma_{new}$

7. Repeat 4 to 6 until converged

REFERENCES

1. Guruswamy, G. P.: ENSAERO—A Multidisciplinary Program for Fluid/Structural Interaction Studies of Aerospace Vehicles. Computing Systems Engineering, vol. 1, 1990, pp. 237–256.

2. Guruswamy, G. P.: Unsteady Aerodynamic and Aeroelastic Calculations for Wings Using Euler Equations. AIAA J., vol. 28, 1990, pp. 461–469.

3. Guruswamy, G. P.: Navier-Stokes Computations on Swept-Tapered Wings, Including Flexibility. AIAA Paper 90-1152, Apr. 1990.

4. Obayashi, S.; Guruswamy, G. P.; and Goorjian, P. M.: Application of Streamwise Upwind Algorithm for Unsteady Transonic Computations over Oscillating Wings. AIAA Paper 90-3103, Aug. 1990.

5. Obayashi, S.; and Guruswamy, G. P.: Unsteady Shock-Vortex Interaction on a Flexible Delta Wing. AIAA Paper 91-1109, Apr. 1991.

6. Obayashi, S.; and Guruswamy, G. P.: Navier-Stokes Computations for Oscillating Control Surface. AIAA Paper 92-4431, Aug. 1992.

7. Obayashi, S.; Guruswamy, G. P.; and Tu, E. L.: Unsteady Navier-Stokes Computations on a Wing-Body Configuration in Ramp Motions. AIAA Paper 91-2865, Aug. 1991.

8. Guruswamy, G. P.: Coupled Finite-Difference/Finite-Element Approach for Wing-Body Aeroelasticity. AIAA Paper 92-4680, Sep. 1992.

9. Guruswamy, G. P.; Weeratunga, S.; and Pramono, E.: Direct Coupling Approach to Fluids/Structures Interaction Problems for Parallel Computing. NASA CAS Conference, Moffett Field, CA 94035-1000, Aug. 18-20, 1992, pp. 46–47.

10. Barszcz, E.: Intercube Communication on the iPSC/860. Proceedings of the Scalable High Performance Computing Conference, Williamsburg, VA, April 26-29, 1992, pp. 307–313.

11. Peyret, R.; and Viviand, H.: Computation of Viscous Compressible Flows Based on Navier-Stokes Equations. AGARD AG-212, 1975.

12. Obayashi, S.; Guruswamy, G. P.; and Goorjian, P. M.: Streamwise Upwind Algorithm for Computing Unsteady Transonic Flows Past Oscillating Wings. AIAA J., vol. 29, 1991, pp. 1668–1677.

15

13. Beam, R.; and Warming, R. F.: An Implicit Finite-Difference Algorithm for Hyperbolic Systems in Conservation Law Form. J. Computational Physics, vol. 22, 1976, pp. 87–110.

14. Pulliam, T. H.; and Chaussee, D. S.: A Diagonal Form of an Implicit Approximate Factorization Algorithm. J. Computational Physics, vol. 39, no. 2, 1981, pp. 347–363.

15. Guruswamy, P.; and Yang, T. Y.: Aeroelastic Time-Response Analysis of Thin Airfoils by Transonic Code LTRAN2. Computers and Fluids, vol. 9, 1980, pp. 409–425.

16. Newmark, N. M.: A Method of Computation for Structural Dynamics. A.S.C.E., J. Engineering Mechanics Division, vol. 85, 1959, pp. 67–94.

17. Harder, R. L.; and Desmarais, R. N.: Interpolation Using Surface Spline. J. Aircraft, vol. 9, 1972, pp. 189–191.

18. Appa, K.: Finite-Surface Spline. J. Aircraft, vol. 26, 1989, pp. 495–496.

19. Pidaparti, R. M. V.: Structural and Aerodynamic Data Transformation Using Inverse Isoparametric Mapping. J. Aircraft, vol. 29, 1992, pp. 507–509.

20. Appa, K.; Yankulich, M.; and Cowan, D. L.: The Determination of Load and Slope Transformation Matrices for Aeroelastic Analyses. J. Aircraft, vol. 22, 1985, pp. 734–736.

21. Ryan, J. S.; and Weeratunga, S. K.: Parallel Computation of 3-D Navier-Stokes Flowfields for Supersonic Vehicles. AIAA Paper 93-0064, Jan. 1993.

22. Law, K. H.: A Parallel Finite Element Solution Method. Computers and Structure, vol. 23, 1986, pp. 845–858.

23. Dogget, R. V.; Rainey, A. G.; and Morgan, H. G.: An Experimental Investigation of Aerodynamics Effects of Airfoil Thickness on Transonic Flutter Characteristics. NASA TM X-79, 1959.

24. Park, K. C.; Pramono, E.; Stanley, G. M.; and Cabiness, H. A.: The ANS Shell Elements: Earlier Developments and Recent Improvements. In Analytical and Computational Models of Shells, A. K. Noor (ed.), CED–Vol. 3, ASME, New York, 1989, pp. 217–240.

25. Bathe, K.-J.: Finite Element Procedures in Engineering Analysis. Prentice-Hall, Englewood Cliffs, New Jersey, 1982, pp. 702–706.
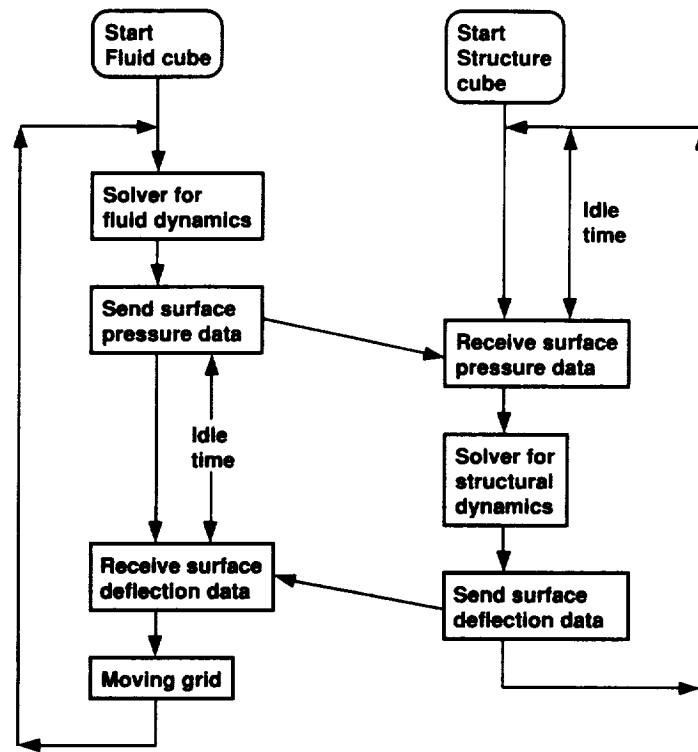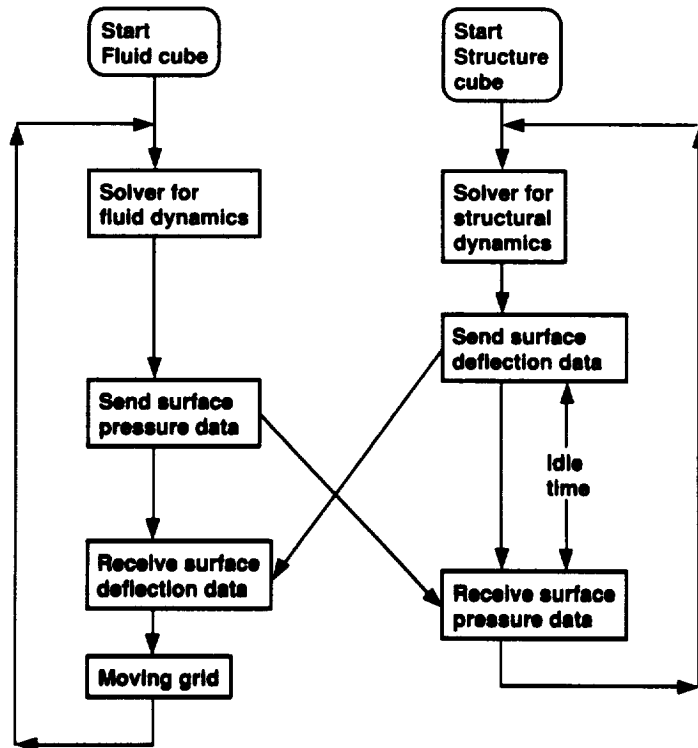
3-D uni-partitioning
(Fluid domain)

Intercube
communication

2-D uni-partitioning
(Structural domain)
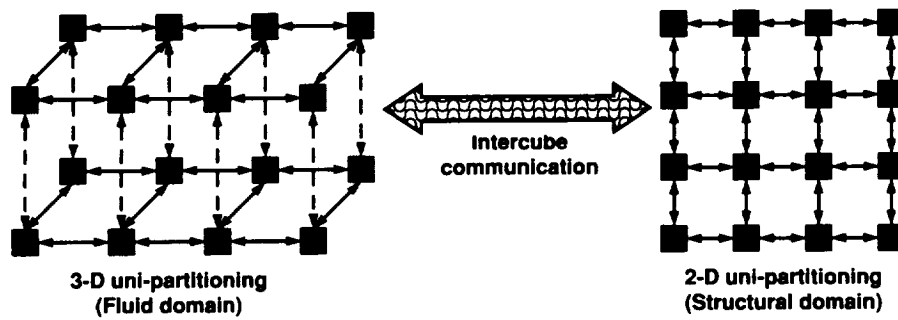
Figure 1. Processor arrangements and message exchanges through interprocessor and intercube communications.

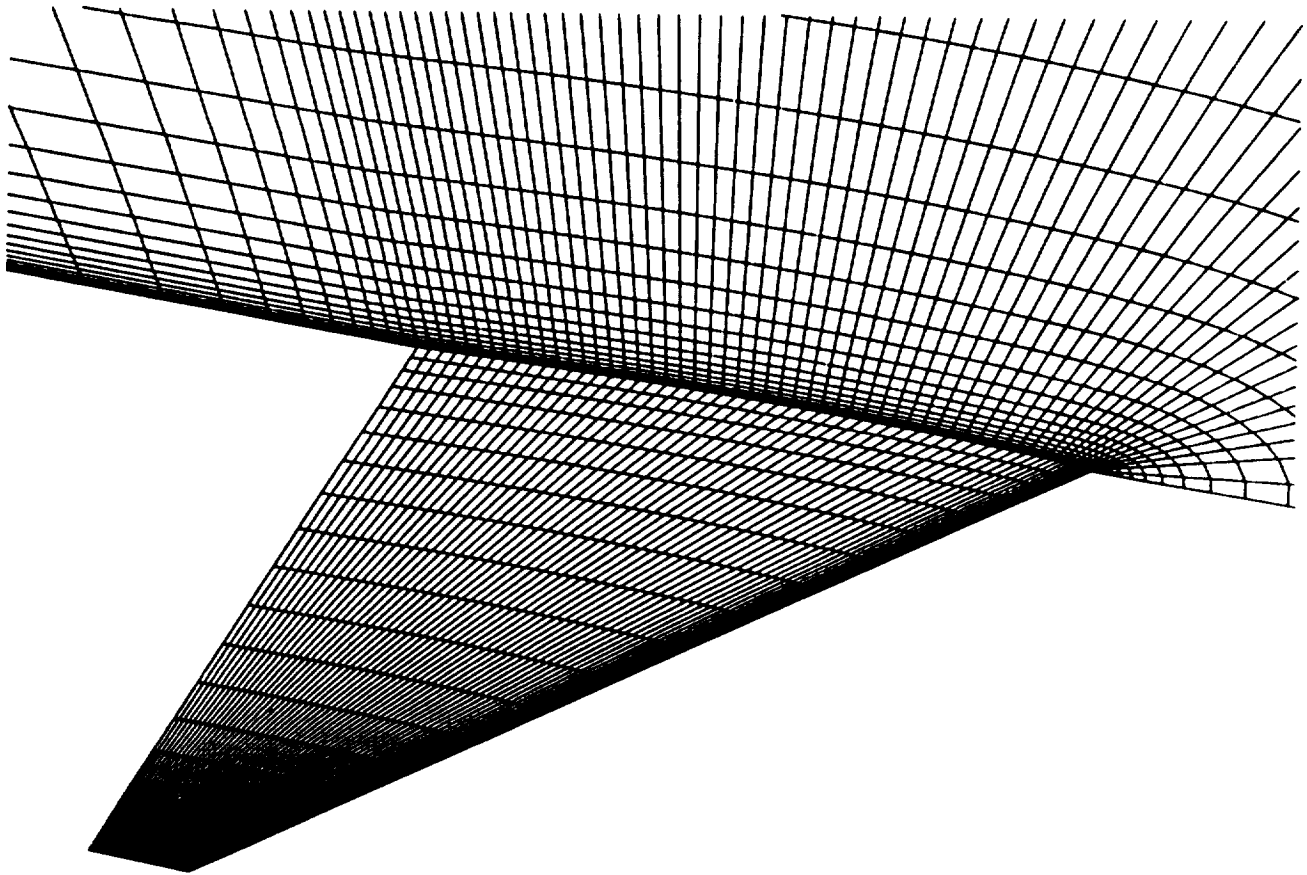Figure 2. Flow diagrams for sequential and parallel integration schemes.

Figure 3. The CFD grid at the root and surface of a clipped delta wing with the NACA 65A006 airfoil section. (Aspect ratio = 3.0, Taper ratio = 1/7, $\Lambda_{c/4} = 45°$)
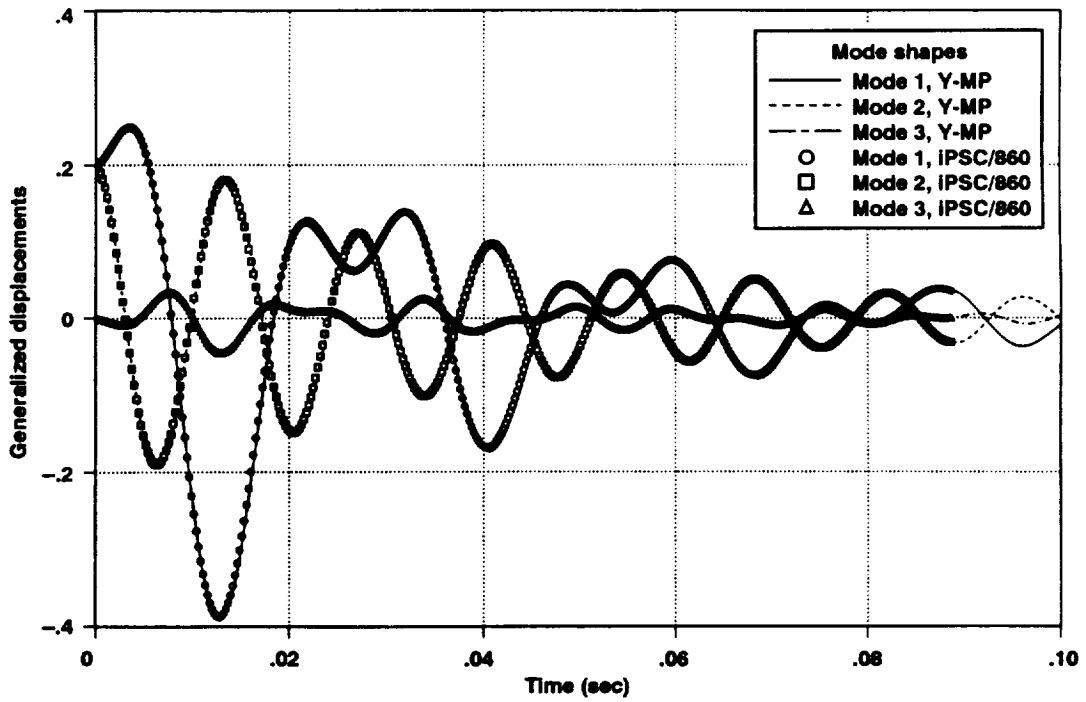
Figure 4. Comparison among the first three generalized displacement histories obtained by the serial and parallel ENSAERO codes. ($M_\infty = 0.854$, P = 0.70 psi)
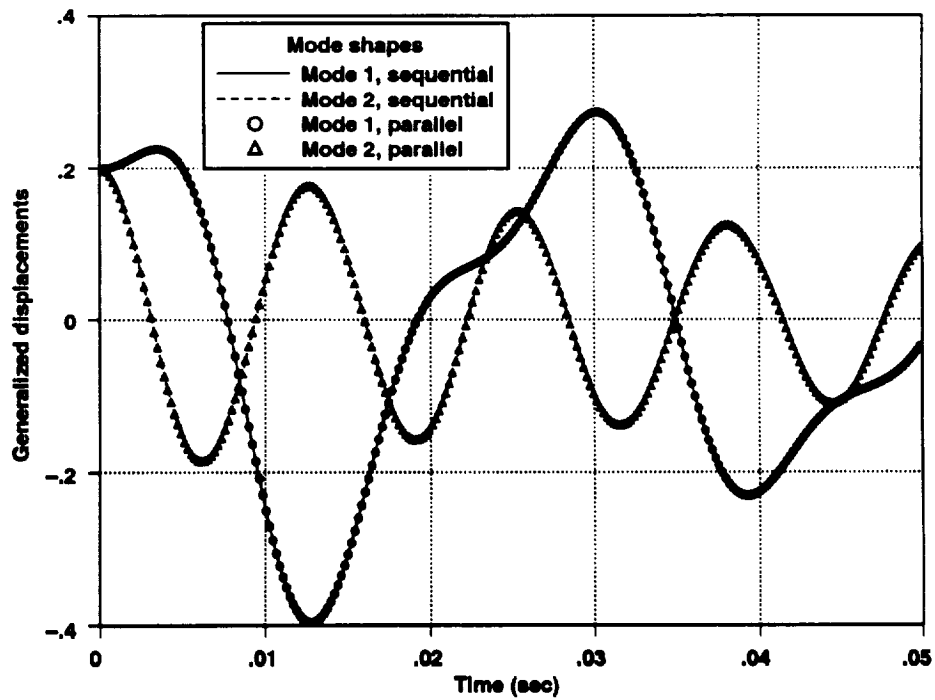
Figure 5. Generalized displacement histories obtained from sequential and parallel integration schemes. ($M_\infty = 0.977$, P = 0.65 psi)

20
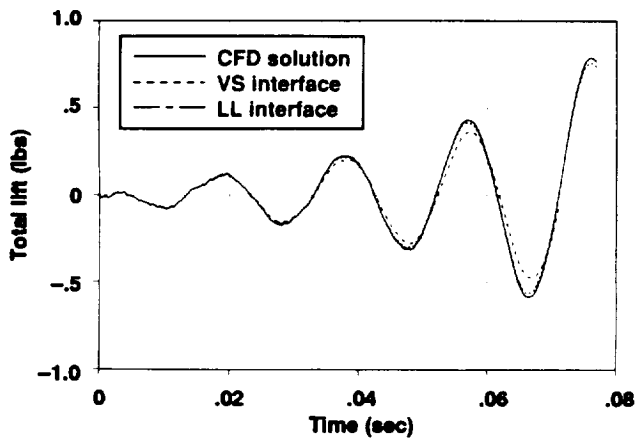
Figure 6. Comparison of total lift responses. ($M_\infty = 0.854$, $\alpha = 0$ deg., P = 1.0 psi)
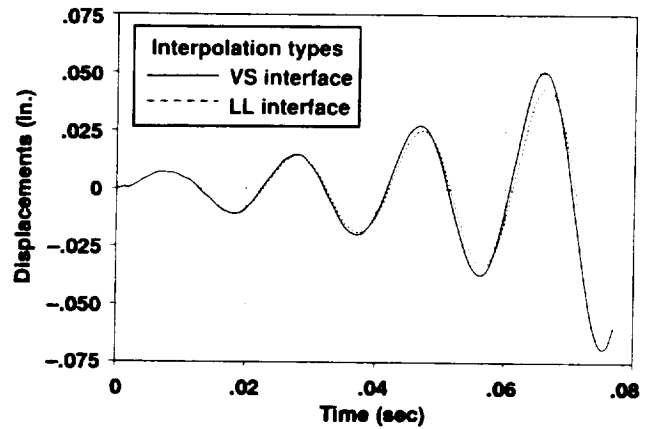
Figure 7. Comparison of wing tip displacements at the leading edge obtained by using virtual surface and lumped load interfaces. ($M_\infty = 0.854$, $\alpha = 0$ deg., P = 1.0 psi)
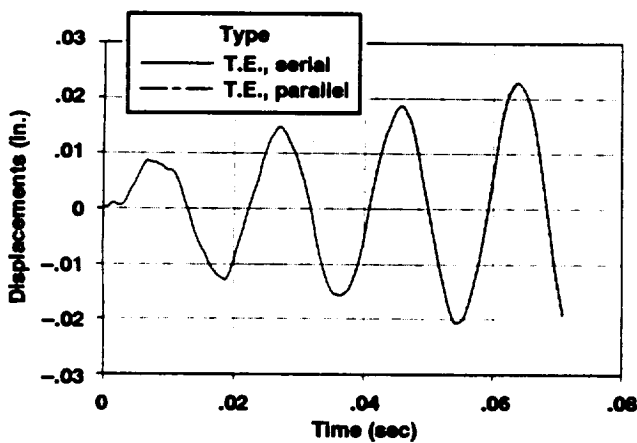
Figure 8. Aeroelastic responses obtained by using sequential and parallel integration schemes. ($M_\infty = 0.854$, $\alpha = 0$ deg., P = 1.0 psi)
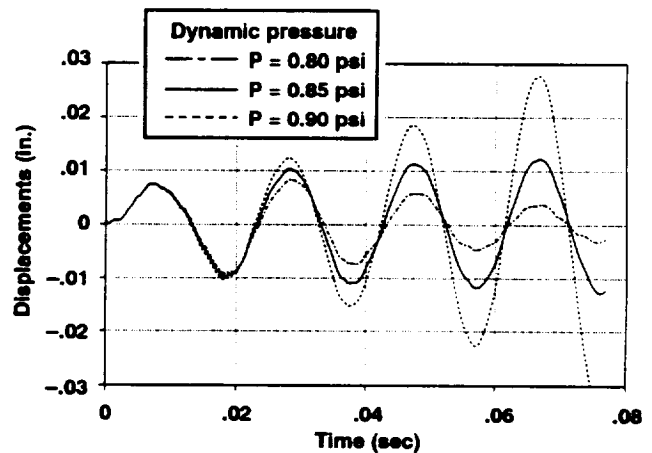

Figure 9. Aeroelastic responses of a clipped delta wing at three different dynamic pressures using Euler equations for the fluid and finite element equations for the structural domains. ($M_\infty = 0.854$, $\alpha = 0$ deg.)
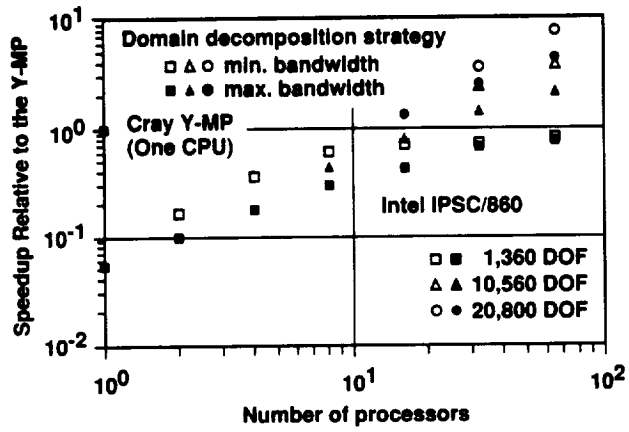
21

Figure 10. Computational performance of the structural domain in ENSAERO with various problem sizes and domain decompositions on the Intel iPSC/860.
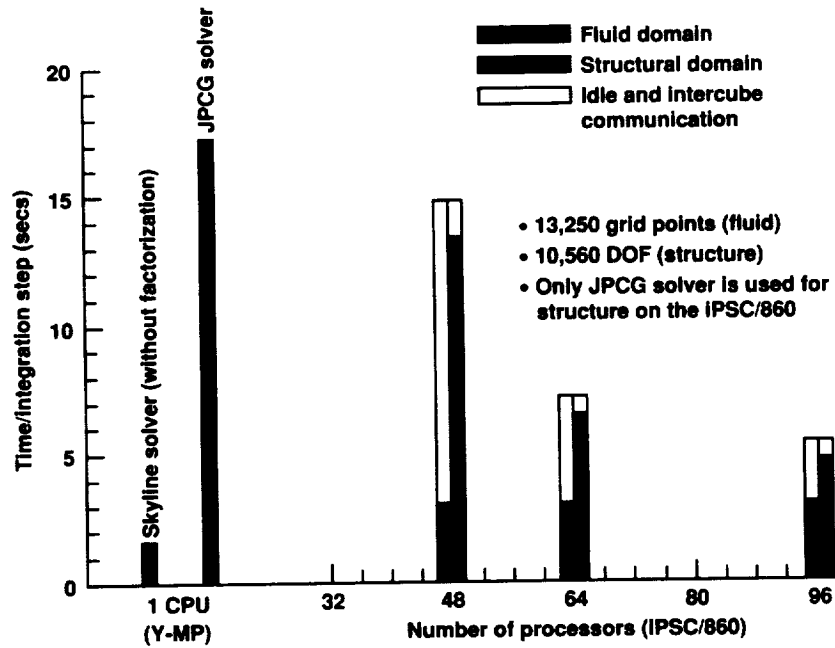

Figure 11. Overall computational performance of ENSAERO on the Cray Y-MP and the Intel iPSC/860.

APPENDIX C.

AIAA-94-1487

Wing-Body Aeroelasticity Using Finite-Difference Fluid/ Finite-Element Structural Equations on Parallel Computers

C. Byun and G. P. Guruswamy
NASA Ames Research Center
Moffett Field, CA

**AIAA/ASME/ASCE/AHS/ASC
35th Structural, Structural Dynamics,
and Materials Conference**
April 18-20, 1994
Hilton Head, SC

WING-BODY AEROELASTICITY USING FINITE-DIFFERENCE FLUID/ FINITE-ELEMENT STRUCTURAL EQUATIONS ON PARALLEL COMPUTERS

Chansup Byun[*] and Guru P. Guruswamy[**]
Computational Aerosciences Branch
NASA Ames Research Center, Moffett Field, California 94035-1000

Abstract

This paper presents a procedure for computing the aeroelasticity of wing-body configurations on multiple-instruction, multiple-data (MIMD) parallel computers. In this procedure, fluids are modeled using Euler equations discretized by a finite difference method, and structures are modeled using finite element equations. The procedure is designed in such a way that each discipline can be developed and maintained independently by using a domain decomposition approach. A parallel integration scheme is used to compute aeroelastic responses by solving the coupled fluid and structural equations concurrently while keeping modularity of each discipline. The present procedure is validated by computing the aeroelastic response of a wing and comparing with experiment. Aeroelastic computations are illustrated for a High Speed Civil Transport type wing-body configuration.

Introduction

The analysis of aeroelasticity involves solving fluid and structural equations together. Both uncoupled and coupled methods can be used to solve problems in aeroelasticity associated with nonlinear systems.[1] Uncoupled methods are less expensive but are limited to very small perturbations with moderate nonlinearity. However, aeroelastic problems of aerospace vehicles are often dominated by large structural deformations and high flow nonlinearities. Fully coupled procedures are required to solve such aeroelasticity problems accurately.

Such coupling procedures result in an increased level of complication. Therefore, aeroelastic analysis has been mostly performed by coupling advanced computational fluid dynamics (CFD) methods with simple structural modal equations or advanced computational structural dynamics (CSD) methods with simple flow

---

* Research Scientist, MCAT Institute, AIAA Member
** Research Scientist, AIAA Associate Fellow

solutions. However, these approaches can be less accurate for the aeroelastic analysis of practical problems such as a full aircraft configuration in transonic regime. It is necessary to develop a fully coupled procedure utilizing advanced computational methods for both disciplines.

Recently, coupled fluid-structural interaction problems are being studied using finite-difference Euler or Navier-Stokes flow equations and finite-element structural equations of motion as demonstrated by an aeroelastic code ENSAERO.[2,3] However, applications are limited to simple structural models. For the complicated fluid and structural models, computations are performed in a step-by-step fashion.[4] The main reason is that the use of detailed models for both disciplines requires unprecedented computing speeds and amounts of memory. The emergence of a new generation of parallel computers can possibly alleviate the restriction on the computational power.

In order to solve the coupled fluid-structural equations, some attempts have been made to solve both fluids and structures in a single computational domain[5,6]. The main defect of this approach is the ill-conditioned matrices associated with two physical domains with large variations in stiffness properties. So far, such attempts have been limited to simple two-dimensional problems.

To overcome the difficulties arising from a single domain approach, the domain decomposition approach reported in Ref. 1 has been incorporated in several advanced aeroelastic codes such as XTRAN3S,[7] ATRANS3S[8] and CAP-TSD[9] based on the transonic small perturbation theory. This domain decomposition approach models fluids and structures independently. The coupling of two disciplines is accomplished by exchanging data at interfaces between fluids and structures. This allows one to take full advantage of numerical procedures for individual disciplines such as finite difference methods for fluids and finite element methods for structures. It was later demonstrated that the same technique can be used for modeling the fluids with Euler/Navier-Stokes equations on moving grids.[10,11] The accuracy of the coupling is maintained by matching the surface grid deformation with the structural displacements at the surface. This new development is incorporated in the computer code ENSAERO.[12] Similar work has also been reported recently in Ref. 13.

For the implementation of the ENSAERO code

on parallel computers, two types of parallel computers were considered. These are the single-instruction, multiple-data (SIMD) and multiple-instruction, multiple-data (MIMD) type computers. However, MIMD type parallel computers are more suitable for computationally efficient implicit solvers and the domain decomposition approach used in the ENSAERO code. By decomposing the computational domain into a number of subdomains and solving an implicit problem on each subdomain, a MIMD computer can reduce the interprocessor communication required for the inversion of a large matrix resulting from an implicit method. Furthermore, a MIMD parallel computer can exploit the parallelism offered by the domain decomposition approach for the coupled fluid and structural disciplines; each computational domain can be treated concurrently. In addition, each fluid and structural algorithms can be designed in a modular fashion on MIMD parallel computers.

In this work, a procedure to compute aeroelasticity on MIMD parallel computers is described. The fluid and structural equations on separate computational domains are coupled by the exchange of interface data. The computational-efficiency issues of parallel integration of both fluid and structural equations are investigated using a parallel version of ENSAERO. The fluid and structural disciplines are modeled using finite-difference (FD) and finite-element (FE) approaches, respectively. The coupled equations are solved using a time integration method with configuration-adaptive moving grids. The procedure is designed in a modular fashion so that each computational discipline can be developed independently and be modified easily. The aeroelastic computations are demonstrated for a High Speed Civil Transport (HSCT) type wing-body configuration on the Intel iPSC/860 parallel computer.

Aeroelastic Computation

The governing aeroelastic equations of motion for structures can be written as

$$[M]\{\ddot{q}\} + [C]\{\dot{q}\} + [K]\{q\} = \{Z\} \qquad (1)$$

where $[M]$, $[C]$, and $[K]$ are the global mass, damping and stiffness matrices, respectively. $\{Z\}$ is the aerodynamic force vector corresponding to displacement vector $\{q\}$. One of the main efforts is computing the aerodynamic force vector $\{Z\}$, which is obtained by solving the fluid flow equations. After obtaining the aerodynamic force, aeroelastic responses can obtained by solving eq. (1). A numerical integration technique based on the constant-average-acceleration method[14] is used to integrate the aeroelastic equations. This is an unconditionally stable scheme.

A domain decomposition approach is selected to solve eq. (1) in conjunction with the flow equations. Each of the fluid and structural equations is modeled in a separate computational domain. Coupling between the fluid and structural equations is accomplished by exchanging boundary interface data at the end of every time step when solving eq. (1). The advantage of this approach is that one can select an efficient algorithm for the fluid domain regardless of the structural domain and vice versa. In this work, a finite difference method is selected for fluids and a finite element method for structures.

In the fluid domain the strong conservation law form of the Euler equations is used to model the flow. To solve the Euler equations, the central-difference scheme based on the implicit approximate factorization algorithm of Beam and Warming[15] with modifications by Pulliam and Chaussee[16] for diagonalization is used. The scheme is first order accurate in time.

To exchange boundary interface data, it is necessary to represent the equivalent aerodynamic loads (i.e. normal stress) at the structural nodal points and to represent the deformed structural configurations at the aerodynamic grid points. Several numerical procedures have been developed to exchange the necessary information between the fluid and structural domains.[17-20]

A node-to-element approach is used to define the location of the points of the fluid surface grid relative to finite elements at the surface of the structure for coupling purposes. In this approach, every grid point of the fluid that lies on the fluid-structural interface is identified with respect to a finite element as shown in Fig. 1. However, in general, it is not straightforward to determine the local coordinate information of each grid point within a finite element. A numerical inverse mapping technique developed by Murti and Valliappan[21] is used to obtain the local coordinate information of all the interface points of the fluid grid with respect to surface elements of the structure. Once the location of each fluid grid point is obtained, the nodal force vector can be easily obtained. Also the deformation of the fluid surface grid is determined by using shape functions of the finite elements used to model the structure. In addition, a linear extrapolation is used to compute the deformation at the points of the fluid surface grid which are not on the surface of the structure, e.g. points at singular planes. Starting from the deformed fluid surface grid, the field grid is generated as explained in a later section.

Parallelization of ENSAERO

The domain decomposition approach enables data structures and solution methods for fluid and structural equations to be developed independently. Fluid

and structural equations are modeled in separate computational domains. Each domain is mapped individually onto a group of processors, referred to as a cube on the Intel iPSC/860, which is selected for this work. The Intel iPSC/860 is a distributed-memory, multiple-instruction, multiple-data (MIMD) computer with 128 processors.

Because of coupling between the two disciplines, the interface boundary data such as surface pressures and structural displacements should be exchanged. This exchange between the fluid and structural domains is accomplished through an intercube communication mechanism.[22] This intercube communication facility enables different processors in each cube on the iPSC/860 to communicate directly.

The fluid flow algorithm solves the Euler equations using 3-D uni-partitioning of the computational domain. The uni-partitioning scheme assigns one subdomain grid to each of the processors. The mapping of subdomain grids to processors is described in Fig. 2. The arrows denote bi-directional data communication. There are a variety of concurrent algorithms available for solving the system of equations for fluids. More details about the implementation of the fluid flow algorithms can be found in Ref. 23.

For the structural domain, regular finite element meshes are used to model the wing and the body as plate and shell structures, respectively. The domain decomposition is made by using 2-D uni-partitioning as shown in Fig. 2. This type of domain decomposition enables an efficient and simple message communication mechanism within the structural domain.

The solver for the structural domain is based on a Jacobi-preconditioned conjugate gradient (JPCG) algorithm on the Intel iPSC/860. The present JPCG algorithm is obtained by implementing the diagonal preconditioner to a parallel conjugate gradient algorithm proposed by Law.[24] In this method, the structural finite element model is divided into subdomains and only local matrices related to the subdomains are assembled. The multiplication of a matrix by a trial vector, which is the major operation of the conjugate gradient algorithm, is performed at the subdomain level. Interprocessor communication is confined to the solution phase, and the communication is only performed between processors which have common finite element nodes.

Aeroelastic Configuration Adaptive Grids

One of the major difficulties in solving the Euler equations for computational aerodynamics lies in the area of grid generation. For steady flows, advanced techniques such as blocked zonal grids[25] are currently being used. However, grid-generation techniques for aeroelastic calculations, which involve moving compo-

nents, are still in the early stages of development. Guruswamy has developed analytical schemes for aeroelastic configuration-adaptive dynamic grids and demonstrated time-accurate aeroelastic responses of wing[10] and wing-body[2,3] configurations.

In this work, an H-O type grid topology is used (H in the streamwise and O in the spanwise directions) for wing-body configurations. This type of grid topology is more suitable for general wing-body configurations. It gives better surface grid resolution on the body when compared to the C-H grid topology used in Ref. 10. The grid is designed such that flow phenomena such as shock-waves, vortices, etc. and their movement around the wing-body configurations are accurately simulated. The base surface grid is prepared using the S3D code.[26] From the surface grid, the field grid is generated using an analytical approach. In this approach, grid lines in the radial direction away from the surface are generated line by line in the planes normal to the longitudinal body axis. First, the radial lines are generated approximately normal to the surface. Then, the new grid lines in the azimuthal direction are generated in such a way that the spacing between lines are exponentially increased away from the surface. This method can be used for generating the base field grid of the rigid configuration and the aeroelastically deformed field grid of the flexible configuration.

Parallelization of this approach is accomplished using the uni-partitioning scheme in the fluid domain. The present approach for aeroelastic configuration-adaptive grids only requires the deformed surface grid and the coefficients used in the exponential function to define the grid spacing between lines away from the surface. So the interprocessor communication needed to generate the deformed field grid within the fluid domain is minimal, and takes place only between processors assigned along the surface-normal direction. Each of the processors can generate the assigned subdomain grid of the deformed field grid concurrently once information about the local surface grid has been broadcast.

The grid is generated at every time step based on the aeroelastically deformed position of the structure. First, the displacements at the points of the fluid surface grid on the structure are obtained on the processors assigned to the structural domain. This is done by using the local coordinate information and the finite element shape functions. The displacements at the points of the fluid surface grid are sent only to the appropriate processors on the fluid domain which contain the surface grid points. Then, a linear extrapolation is used to obtain the displacements at the remaining points of the surface grid, such as the points at singular planes which are not on the surface of the structure. At this stage, the deformed surface grid is distributed only to proces-

sors of the fluid domain which contain the local surface grid points. It should be noted that the deformed surface grid residing on each processor of the fluid domain is only the part of the whole surface grid according to the grid partitioning. If two or more processors are assigned along the surface-normal direction, each of the deformed surface partitions is sent to processors which have the same partitioning indices of the surface grid. Finally, all processors of the fluid domain generate their subdomain of the deformed field grid concurrently.

Parallel Integration for Coupled Domains

In a serial computer, the integration of both fluid and structural equations is performed one after the other in a sequential nature. Figure 3(a) shows the sequential integration scheme implemented on MIMD parallel computers. In the sequential integration scheme, the fluid domain has to wait to proceed to the next time step until it receives information about structural deformations. The structural domain also has to wait for surface pressure data. So, both cubes have their own idle times waiting for data communications. The computational time per integration step will be determined by times spent on both domains when a sequential integration scheme is used. In order to avoid the idle times between the fluid and structural computations, all processors can be used to solve the fluid and structural equations sequentially as done in serial computations. But this approach requires more memory per processor and two disciplines have to be implemented in a single program. As a result, modularity of each algorithm for individual disciplines will have to be sacrificed to a significant degree. In addition, this approach will be less efficient as increasing the number of processors because the problem is not linearly scaled.

However, while keeping modularity of each discipline, computations can be done more efficiently on MIMD parallel computers by executing the integration of both fluid and structural equations concurrently as shown in Fig. 3(b). In the proposed parallel integration scheme, both domains start computations independently and one of the solvers waits until the other finishes its calculation. Then they exchange the required data with each other for the next time step. By doing so, the parallel integration can reduce the idle time since only one cube (the fastest) will have to wait. The resulting speedup by the parallel integration scheme is a factor of almost 2, provided that computational times required for the fluid and structural domains are well balanced. This integration scheme exploit the parallelism offered by the domain decomposition approach to solve the coupled fluid-structural interaction problems.

Results

Wing Aeroelasticity

In order to validate the present development, computations were done for a clipped delta wing configuration.[27] The transonic flutter characteristics of this wing are available from wind tunnel tests for various flow parameters. For this computation, the flow field is discretized using a C-H grid topology of size 151 × 30 × 25. The fluid grid is assigned to 32 processors on the iPSC/860. The processors are arranged as a 3-D mesh of 8 processors in the chordwise direction and 2 processors in both the spanwise and surface-normal directions.

A 20 degrees-of-freedom (DOF) ANS4 shell[28] element was used for the finite element modeling of the structure. The wing is modeled as a plate. Considering the wing model used in the experiment, variation of mass density is allowed along the chordwise and spanwise directions. But the thickness of the finite element model is kept constant. This is based on the assumptions that the stiffness of the wing is dominated by an aluminum-alloy insert and that the mass distribution of the wing is significantly changed due to plastic foams covering the aluminum-alloy insert. For the structures part of the computation, processors were assigned as a 2-D mesh of 2 processors in the chordwise and spanwise directions, respectively, on the iPSC/860.

In order to compare sequential and parallel integration schemes, the aeroelastic responses were obtained using both schemes on the iPSC/860. The results are presented in Fig. 4. The responses were obtained for 0° angle of attack (AoA) at $M_\infty = 0.854$ and a given dynamic pressure of 1.0 psi. The two results agree well. For 256 finite elements (1360 DOF) with 4 processors on the structural domain, the computational times per integration step are 6.22 and 3.33 seconds by using sequential and parallel integration schemes, respectively. A speedup factor of 1.87 is achieved by using the parallel integration scheme. The parallel integration scheme enables concurrent solution of the coupled fluid and structural equations without causing any significant inaccuracy or instability problems. The computation time per integration step required is determined by the computational domain that requires most time per integration step. This parallel integration is one of the advantages of using MIMD computers for multidisciplinary analysis.

Aeroelastic responses were also computed for various other dynamic pressures in order to predict the flutter dynamic pressure and compare with the experiment. Figure 5 shows the stable, near neutrally stable, and unstable responses of wing tip displacements at the leading edge for dynamic pressures of 0.80, 0.85,

and 0.90 psi, respectively. From the responses shown in Fig. 5, the interpolated dynamic pressure for the neutrally stable condition is 0.84 psi. It is noted that the experimental dynamic pressure measured at the neutrally stable condition was 0.91 psi.[27] Considering the lack of experimental pressure data on the wing and the error involved in modeling the wing as a plate with constant thickness, the computational result is deemed an acceptable prediction of the flutter dynamic pressure.

Wing-Body Aeroelasticity

The main purpose of this work is to compute aeroelastic responses of fully flexible wing-body configurations on MIMD parallel computers. For this purpose, a general-purpose moving-grid capability is required. In the present work, an analytical scheme[3] that will generate a moving H-O grid is implemented on the iPSC/860. This scheme generates the field grid according to the surface grid deformation. For demonstration purposes, an HSCT type wing-body configuration (1807 model) is selected. Figure 6 show the baseline grid. The size of the baseline grid is $95 \times 89 \times 30$. However, it should be noted that the technology developed in this work for moving grid is independent of grid size. The grid generated by the code when the structure is deformed is shown in Fig. 7. Note that the singular planes upstream of the leading edge and downstream of the trailing edge are deformed according to the deformed shape of the configuration.

In order to verify the coupling of the surface movement with the grid movement, dynamic aeroelastic responses are obtained for the above wing-body configuration. Both the body and wing are allowed to be flexible. The wing-body configuration is modeled as a plate/shell structure using 308 elements. The finite element layout is shown in Fig. 8. The structural properties are chosen so that the structure can demonstrate aeroelastic responses for a given flow condition. Symmetric boundary conditions are applied at the top and bottom of the body symmetry lines. All DOF are fixed along the bottom symmetry line of the mid-body. This results in a total of 1641 DOF for the structure.

Aeroelastic computations are done on the flexible wing-body configuration by directly coupling the pressures computed solving the Euler equations with the FE structural equations of motion. A demonstration calculation is done for a dynamic aeroelastic case when the configuration is ramping up from 0° to 5° AoA at $M_\infty = 2.1$ as shown in Fig. 9. This ramping motion is started from the steady state of 4.75° AoA and $M_\infty = 2.1$. It is assumed that the wing root is 300 inches long and aeroelastic computations are done at a dynamic pressure of 3.0 psi. The configuration is pitched up about the axis perpendicular to the symmetry plane and located at the leading edge of the wing root. Starting from the steady state solution, the configuration is pitched up at a rate of 0.0015 degrees per time step. At the end of each time step a new field grid is generated that conforms to the deformed surface. Figure 9 shows the response of the leading edge of the tip section. It is noted that the wing continues to oscillate after the ramp motion has stopped. This is because the inertial force on the structure is still dominating the aeroelastic motion.

The effect of aerodynamic forces on the aeroelastic responses is studied as shown in Fig. 10. The computations are started from the steady state solution at 4.75° AoA and $M_\infty = 2.1$ with an initial motion of the structure due to uniform accelerations to simulate gust loads. When aerodynamic forces are not applied, the structure is oscillating without decrease in amplitude. But the magnitude of the wing tip deflection is negligible. Upon applying aerodynamic forces, the wing tip deflection becomes significant. However, the aerodynamic damping reduces the amplitude of the structural responses gradually.

Performance

In order to measure the performance of the structural domain on the Intel iPSC/860, the FLOP (floating-point operations) rate on the iPSC/860 is calculated by comparing time per integration step on the iPSC/860 to the time on the Y-MP using a single processor. Operation counts from the Cray Hardware Performance Monitor are used. A single processor of the iPSC/860 achieve the Y-MP equivalent of 4.2 MFLOPS, while the corresponding rate is about 77 MFLOPS on a single Y-MP processor. The Intel rate is about 7 percent of the peak performance of a single processor on the iPSC/860. Similar performance was reported by Ryan and Weeratunga[21] for the fluid domain. All performance data reported are for 64-bit arithmetic.

The performance of the structural domain in parallel ENSAERO has been measured over a wide range of processor numbers and problem sizes as shown in Fig. 11. The speedup relative to the Y-MP is defined as

$$speedup = \frac{t_{Cray}}{t_{Intel}}$$

where t_{Cray} and t_{Intel} are the computational time per integration step measured on the Y-MP and the iPSC/860, respectively. Only a single processor is used to measure t_{Cray} on the Y-MP. The open and filled symbols denote the domain decomposition approach which results in the minimum and maximum bandwidths of the stiffness matrix of each subdomain for a given number of processors, respectively.

For the case of 1,360 DOF, the computational time per integration step for 64 processors on the iPSC/860 is close to that on the Y-MP. However, by increasing the size of the problem (10,560 and 20,800 DOF), 16 processors of the iPSC/860 achieve about the same speed as a single Y-MP processor. It is evident that the JPCG solver on the iPSC/860 performs better as the size of problem increases. For the case of 20,800 DOF, the relative speedup achieved is about 8 when 64 processors are in use on the iPSC/860.

The overall performance of ENSAERO on both the Y-MP and the iPSC/860 is shown in Fig. 12 for the case of 113,250 grid points for the fluid domain and 10,560 DOF for the structural domain. In this computation, 32 processors are assigned to the fluid domain and 16 to 64 processors to the structural domain. Both the skyline reduction and JPCG solvers are compared on the Y-MP while only the JPCG solver is used for the structural domain. The height of each column stands for the time per integration step. Each column is divided into times spent for the fluid domain, the structural domain, and for idle/intercube communication.

For the structural domain, it is evident that the skyline reduction solver outperforms the JPCG solver on the Y-MP. However, the JPCG solver is first implemented on the iPSC/860. Direct solvers are still under development on parallel computers. The main purpose of this work is to compute aeroelastic responses of aerospace vehicles on MIMD parallel computers. Therefore the well-developed JPCG solver is selected. Due to the domain decomposition approach used in this work, the JPCG solver can be easily replaced with more efficient solvers when they become available.

When using 32 processors for the structural domain, the JPCG solver on the iPSC/860 achieves the performance of the skyline reduction solver on the Y-MP. The time per integration step of ENSAERO using 96 processors in total on the iPSC/860 is about 60% of that obtained using the skyline reduction solver with a single processor on the Y-MP. This result is based on the computation time for the case of 113,250 CFD grid points and 10,560 structural equations. It should be noted that the structural domain determined the time per integration step for this particular problem on the iPSC/860. Most of the time on the fluid domain was spent waiting for the interface boundary data. However, due to the domain decomposition approach, it is possible to balance the computational time between the two domains by assigning more processors to the structural domain.

Conclusions

A parallel wing-body version of a multidisciplinary code, ENSAERO, has been developed on the Intel iPSC/860. A domain decomposition approach was used to enable algorithms for the fluid and structural disciplines to be developed and maintained independently. This approach provides an efficient and effective environment to researchers. A researcher working in the fluid or the structural discipline can develop his own algorithms independent of the others. Coupling of the disciplines is achieved by exchanging boundary data through an intercube communication mechanism. This makes it easy for each discipline to incorporate and develop new algorithms or data structures without interferences.

The performance of the structural domain is far behind that of the fluid domain. This is due to the less desirable performance of the JPCG algorithm. It is noted that direct solvers are still in the early stages of development. However, since the procedure developed here allows for one domain to select algorithms independent of others, the JPCG algorithm can be easily replaced with more efficient algorithms when available. Although the solver for the structure is not efficient on a serial computer, reasonable computational speed and a good load balance can be achieved by assigning more processors to the structural domain. The overall time per integration step of parallel ENSAERO using 96 processors on the iPSC/860 is reduced to about 60% of the best time obtained on a single Y-MP processor for the particular problem considered. This shows the advantage of using the domain decomposition approach for the multidisciplinary analysis on MIMD parallel computers.

The parallel integration scheme enables the combination of advanced CFD and CSD technologies with minimal increase in computational time per integration step while keeping modularity of each discipline. The time per integration step is solely determined by the domain that requires most computational time on the iPSC/860. This parallel integration is one of the advantages of using MIMD computers for multidisciplinary analysis. The procedure developed in this research will provide an efficient tool for solving aeroelastic problems of complete aerospace vehicle configurations on MIMD computers.

Acknowledgments

References

1 Guruswamy, P. and Yang, T. Y., "Aeroelastic Time-Response Analysis of Thin Airfoils by Transonic Code LTRAN2," *Computers and Fluids*, Vol. 9, No. 4, Dec. 1980, pp. 409–425.

2 Guruswamy, G. P., "Coupled Finite-Difference/ Finite-Element Approach for Wing-Body Aeroelasticity," AIAA Paper 92-4680, Sep. 1992.

3 Guruswamy, G. P. and Byun, C., "Fluid-Structural Interactions Using Navier-Stokes Flow Equations Coupled with Shell Finite Element Structures," AIAA Paper 93-3087, July 1993.

4 Weaver, M. A., Gramoll, K. C. and Roach, R. L., "Structural Analysis of a Flexible Structural Member Protruding into an Interior Flow Field," AIAA paper 93-1446, April 1993.

5 Bendiksen, O. O., "A New Approach to Computational Aeroelasticity," AIAA-91-0930-CP, Baltimore, MD, April 1991, pp. 1712–1727.

6 Felker, F. F., "A New Method For Transonic Static Aeroelastic Problems," AIAA-92-2123-CP, Dallas, Texas, April 1992, pp. 415–425.

7 Borland, C. J. and Rizzetta, D., "XTRAN3S - Transonic Steady and Unsteady Aerodynamics for Aeroelastic Applications, Volume I-Theoretical Manual," AFWAL-TR-80-3107, Dec. 1985.

8 Guruswamy, G. P., Goorjian, P. M., and Merritt, F. J., "ATRAN2S-An Unsteady Transonic Code for Clean Wings," NASA TM 86783, Dec. 1985.

9 Batina, J. T., Bennett, R. M., Seidal, D. A., Cunningham, S. R., and Bland, S. R., "Recent Advances in Transonic Computational Aeroelasticity," NASA TM 100663, Sept. 1988.

10 Guruswamy, P., "Unsteady Aerodynamics and Aeroelastic Calculations of Wings Using Euler Equations," *AIAA J.*, Vol. 28, No. 3, March 1990, pp. 461–469.

11 Guruswamy, G. P., "Vortical Flow Computations on a Flexible Blended Wing-Body Configuration," *AIAA J.*, Vol. 30, No. 10, Oct. 1992, pp. 2497–2503.

12 Guruswamy, G. P., "ENSAERO-A Multidisciplinary Program for Fluid/Structural Interaction Studies of Aerospace Vehicles," *Computing System Engineering*, Vol. 1, Nos. 2-4, 1990, pp. 237–256.

13 Lee-Rausch, E. M. and Batina, J. T., "Calculation of AGARD Wing 445.6 Flutter Using Navier-Stokes Aerodynamics," AIAA-93-3476, 11th Applied Aerodynamics Conf., Monterey, CA, Aug. 1993.

14 Newmark, N. M., "A Method of Computation for Structural Dynamics," *A.S.C.E., J. of Engineering Mechanics Division*, Vol. 85, 1959, pp. 67–94.

15 Beam, R. and Warming, R. F., "An Implicit Finite-Difference Algorithm for Hyperbolic Systems in Conservation Law Form," *J. of Computational Physics*, Vol. 22, No. 9, Sept. 1976, pp. 87–110.

16 Pulliam, T. H. and Chaussee, D. S., "A Diagonal Form of an Implicit Approximate Factorization Algorithm," *J. of Computational Physics*, Vol. 39, No. 2, Feb. 1981, pp. 347–363.

17 Harder, R. L. and Desmarais, R. N., "Interpolation Using Surface Spline," *J. of Aircraft*, Vol. 9, Sept. 1972, pp. 189–191.

18 Appa, K., Yankulich, M. and Cowan, D. L., "The Determination of Load and Slope Transformation Matrices for Aeroelastic Analysis," *J. of Aircraft*, Vol. 22, 1985, pp. 734–736.

19 Appa, K., "Finite-Surface Spline," *J. of Aircraft*, Vol. 26, 1989, pp. 495–496.

20 Pidaparti, R. M. V., "Structural and Aerodynamic Data Transformation Using Inverse Isoparametric Mapping," *J. of Aircraft*, Vol. 29, 1992, pp. 507–509.

21 Murti, V. and Valliappan, S., "Numerical Inverse Isoparametric Mapping in Remeshing and Nodal Quantity Contouring," *Comp. and Struc.*, Vol. 22, No. 6, 1986, pp. 1011–1021.

22 Barszcz, E., "Intercube Communication on the iPSC/ 860," Proceedings of the Scalable High Performance Computing Conference, Williamsburg, VA, April 26-29, 1992, pp. 307–313.

23 Ryan, J. S. and Weeratunga, S. K., "Parallel Computation of 3-D Navier-Stokes Flowfields for Supersonic Vehicles," AIAA Paper 93-0064, Jan. 1993.

24 Law, K. H., "A Parallel Finite Element Solution Method," *Comp. and Struc.*, Vol. 23, 1986, pp. 845–858.

25 Holst, T. L., Flores. J., Kaynak, U., and Chaderjian, N., "Navier-Stokes Computations, Including a Complete F-16 Aircraft," Chapter 21, Applied Computational Aerodynamics, edited by P. A. Henne, Vol. 125, *Progress in Astronautics and Aeronautics*, AIAA, ISBN 0-930403-69-X, 1990.

26 Luh, R. C., Pierce, L. and Yip, D., "Interactive Surface Grid Generation," AIAA Paper 91-0796, Reno Nevada, Jan. 1991.

27 Dogget, R. V., Rainey, A. G. and Morgan, H. G., "An Experimental Investigation of Aerodynamics Effects of Airfoil Thickness on Transonic Flutter Characteristics," NASA TM X-79, 1959.

28 Park, K. C., Pramono, E., Stanley, G. M. and Cabiness, H. A., "The ANS Shell Elements: Earlier Developments and Recent Improvements," Analytical and Computational Models of Shells, Edited by Noor, A. K., CED-Vol. 3, ASME, New York, 1989, pp. 217–240.
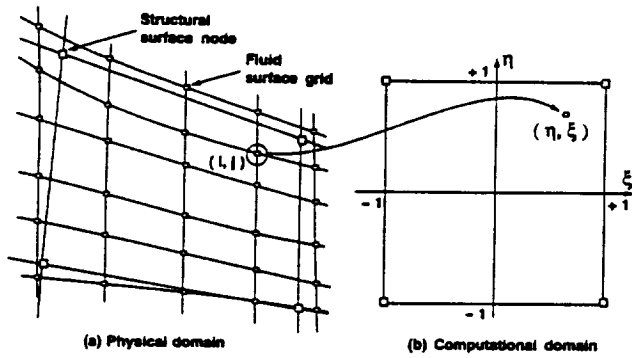
(a) Physical domain   (b) Computational domain

Fig. 1: A schematic diagram of the node-to-element approach for the fluid-structural interface.

3-D uni-partitioning
(Fluid domain)
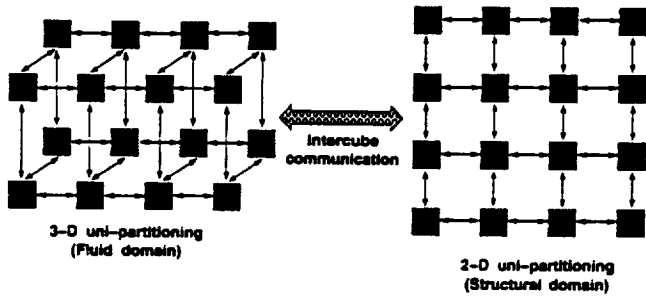
2-D uni-partitioning
(Structural domain)

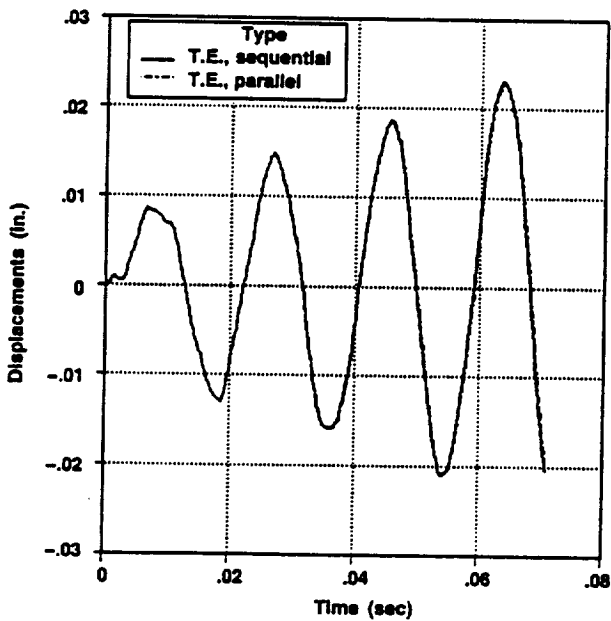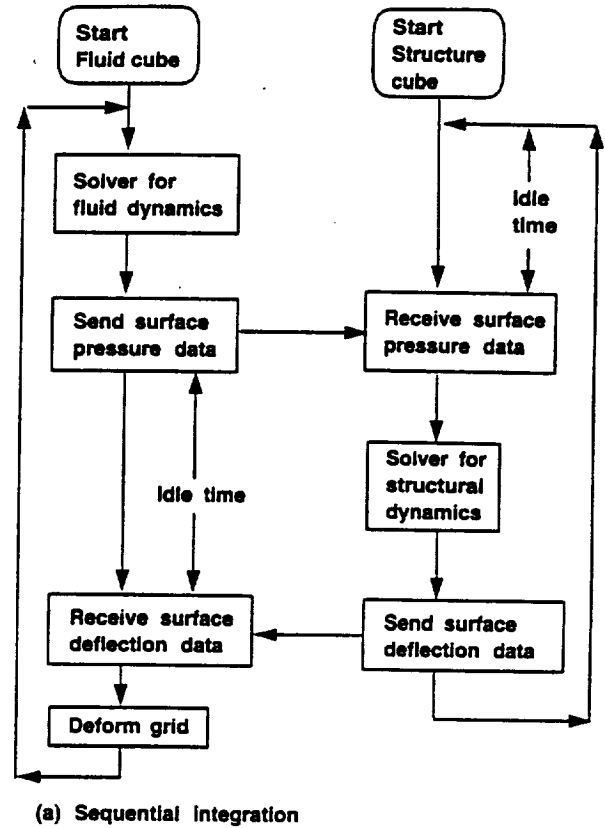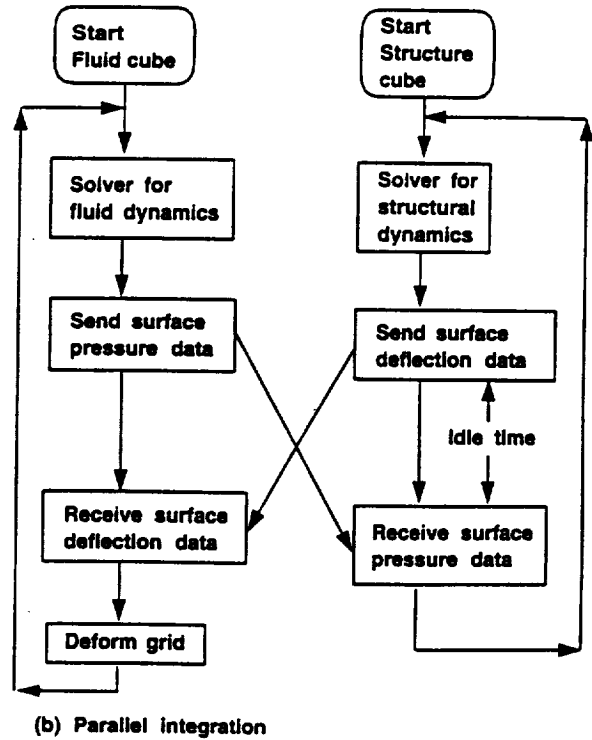**Fig. 2:** Processor arrangements and message exchanges through interprocessor and intercube communications.

Fig. 4: Aeroelastic responses obtained by using sequential and parallel integration schemes. ($M_\infty = 0.854$, $\alpha = 0°$, P= 1.0 psi)

(a) Sequential integration

(b) Parallel integration

Fig. 3: Flow diagrams for sequential and parallel integration schemes.
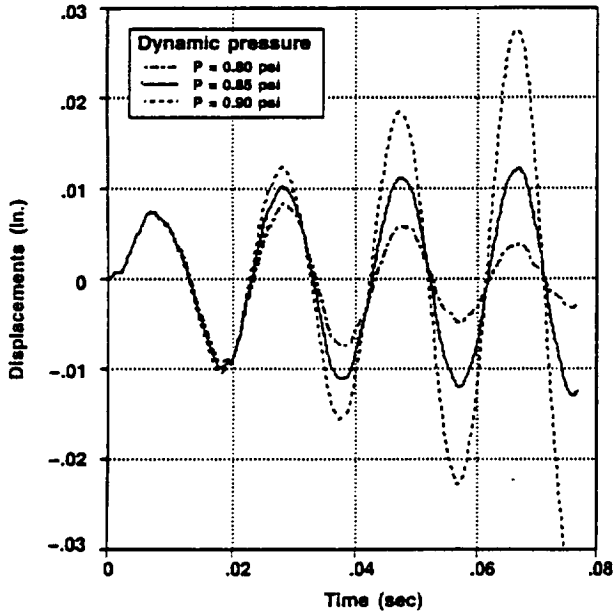
Fig. 5: Aeroelastic responses of a clipped delta wing obtained by solving finite-difference Euler equations and finite-element structural equations of motion. ($M_\infty = 0.854$, $\alpha = 0°$)
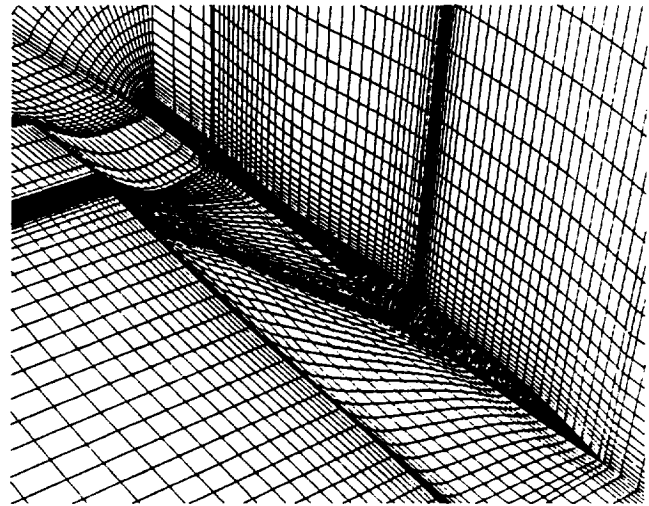
Fig. 7: Deformed surface and field grids.
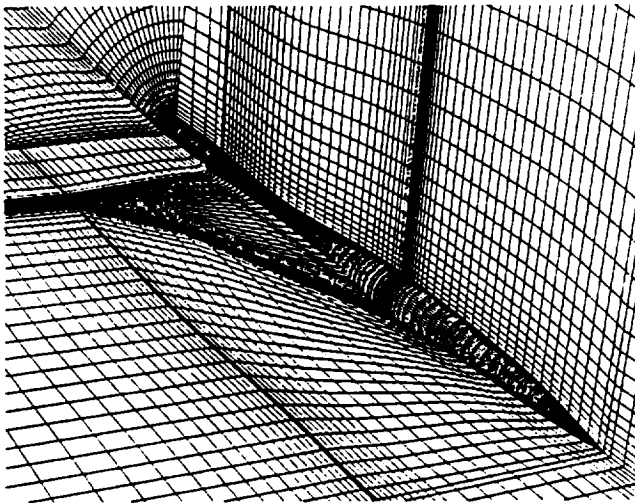
Fig. 6: An HSCT type wing-body configuration with portions of surface and field physical grids.
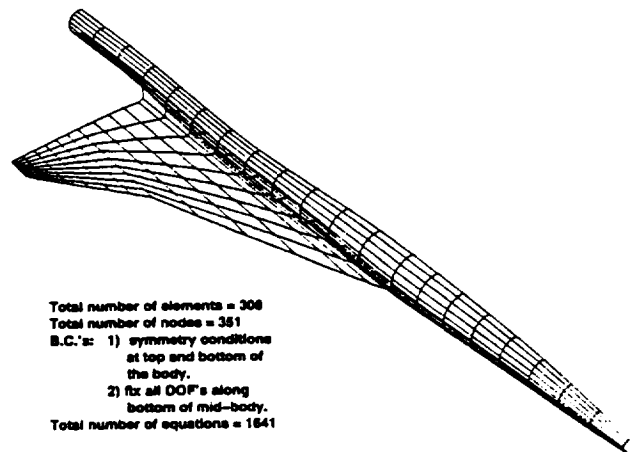
Fig. 8: Finite-element modeling of the wing-body configuration.
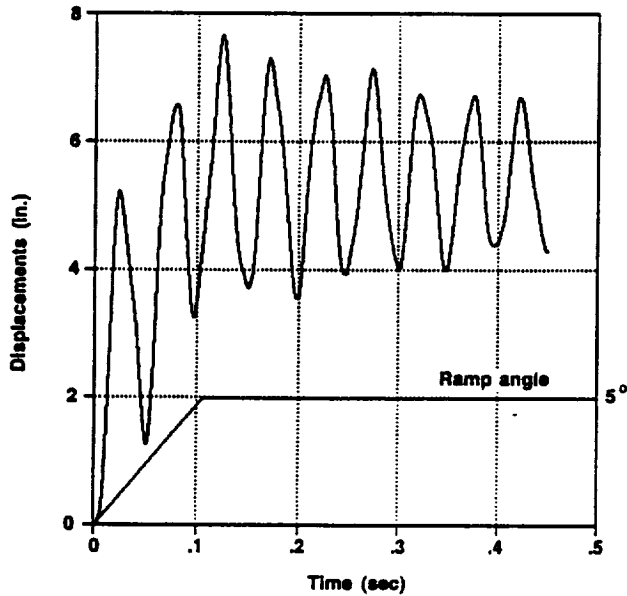
Fig. 9: Dynamic aeroelastic displacements at the wing-tip leading edge of an HSCT type wing-body with ramp motion. ($M_\infty = 2.1$, $\alpha = 4.75°$, P= 3.0 psi)

Fig. 11: Computational performance of the structural domain in ENSAERO with various problem sizes and domain decompositions on the Intel iPSC/860
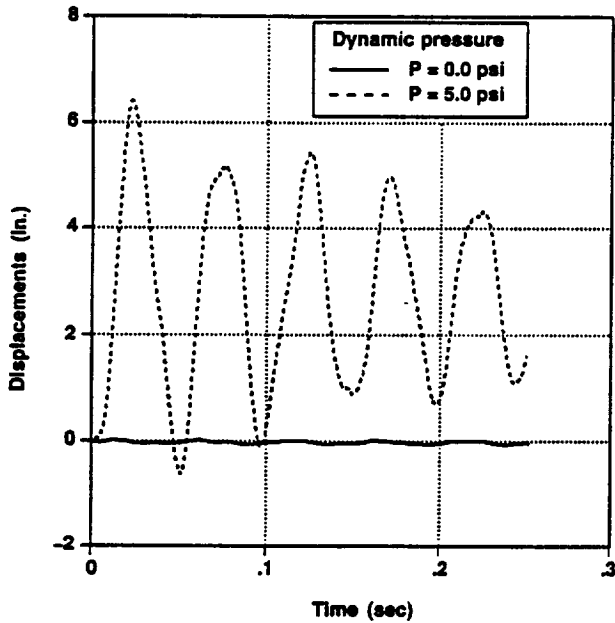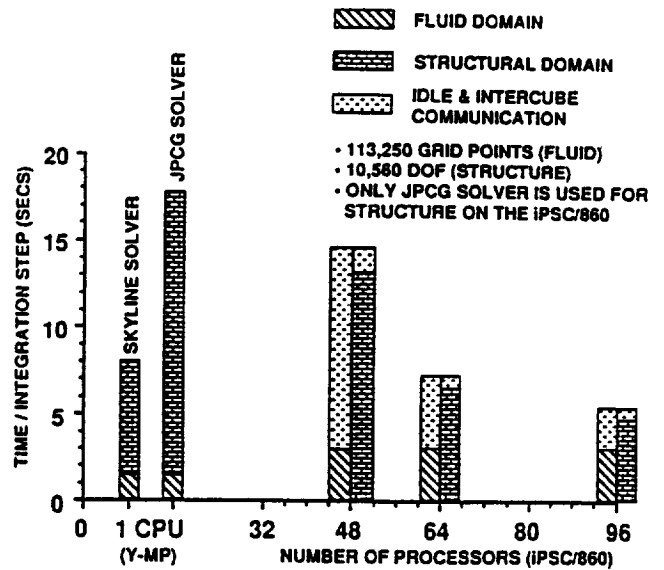

Fig. 10: Effect of aerodynamic forces on the aeroelastic responses of an HSCT type wing-body. ($M_\infty = 2.1$, $\alpha = 4.75°$)

Fig. 12: Overall computational performance of EN-SAERO on the Cray Y-MP and the Intel iPSC/860.

REPORT DOCUMENTATION PAGE

1. AGENCY USE ONLY (Leave blank)	2. REPORT DATE January 1994	3. REPORT TYPE AND DATES COVERED Technical Memorandum

4. TITLE AND SUBTITLE

A Comparative Study of Serial and Parallel Aeroelastic Computations of Wings

5. FUNDING NUMBERS

505-10-11

6. AUTHOR(S)

Chansup Byun and Guru P. Guruswamy

7. PERFORMING ORGANIZATION NAME(S) AND ADDRESS(ES)

Ames Research Center
Moffett Field, CA 94035-1000

8. PERFORMING ORGANIZATION REPORT NUMBER

A-94039

9. SPONSORING/MONITORING AGENCY NAME(S) AND ADDRESS(ES)

National Aeronautics and Space Administration
Washington, DC 20546-0001

10. SPONSORING/MONITORING AGENCY REPORT NUMBER

NASA TM-108805

11. SUPPLEMENTARY NOTES

Point of Contact: Byun Chansup, Ames Research Center, MS 258-2, Moffett Field, CA 94035-1000;
(415) 604-4526

12a. DISTRIBUTION/AVAILABILITY STATEMENT

Unclassified — Unlimited
Subject Category 02

12b. DISTRIBUTION CODE

13. ABSTRACT (Maximum 200 words)

This paper presents a procedure for computing the aeroelasticity of wings on parallel multiple-instruction, multiple-data (MIMD) computers, In this procedure, fluids are modeled using Euler equations, and structures are modeled using modal or finite element equations. The procedure is designed in such a way that each discipline can be developed and maintained independently by using a domain decomposition approach. In the present parallel procedure, each computational domain is scalable. A parallel integration scheme is used to compute aeroelastic responses by solving fluid and structural equations concurrently. The computational efficiency issues of parallel integration of both fluid and structural equations are investigated in detail. This approach, which reduces the total computational time by a factor of almost 2, is demonstrated for a typical aeroelastic wing by using various numbers of processors on the Intel iPSC/860.

14. SUBJECT TERMS

Aeroelasticity, Parallel computation, Wings

15. NUMBER OF PAGES

24

16. PRICE CODE

A03

17. SECURITY CLASSIFICATION OF REPORT Unclassified	18. SECURITY CLASSIFICATION OF THIS PAGE Unclassified	19. SECURITY CLASSIFICATION OF ABSTRACT	20. LIMITATION OF ABSTRACT